Journal of Agriculture and Environment for International Development - JAEID 2025, 119 (2): 59-96
DOI: 10.36253/jaeid-17264

The impact of community-mobilized watershed management interventions on the spatiotemporal erosion patterns and implications: Community Engagement for Erosion Control and Sustainable Watershed Management

HAILU KENDIE ADDIS[1*], TEMESEGEN MULUALEM[2], BEYENE BELAY[3], SIMEGNEW TAMIR[4], SHIGDAF MEKURIAW[4], TADESSE BIREHANU[2], ANTENEH TILAHUN[5], TILAYE TEKLEWOLD[6], ALMAZ GIZIEW ADUGNA[2,3], BELETE ANTENEH[5], YISMAW WULETAW[2], ESMELALEM MHIRET[2], LIKAWENT YEHEYIS[1], HAILEMARIAM KEFYALEW[2], TESFAYE FEYISA[1], MENALE WONDIE[1], AND ASMARE DEJEN[1]

[1] *Amhara Agricultural Research Institute, PO Box. 527, Bahir Dar Ethiopia*

[2] *Amhara Region Bureau of Agriculture, PO Box. 437, Bahir Dar Ethiopia*

[3] *Bahir Dar University, Department of Rural Development and Agricultural Extension, College of Agriculture and Environmental Science, Bahir Dar, Ethiopia*

[4] *Andassa Livestock Research Centre, Amhara Agricultural Research Institute, Bahir Dar, Ethiopia*

[5] *Ethiopian Agricultural Transformation Institute, Amhara Region Agricultural Transformation Office, Bahir Dar Ethiopia*

[6] *Stichting Wageningen Research (SWR) Ethiopia, Wageningen University & Research (WUR), Addis Ababa, P. O. Box 88, Ethiopia.*

**Correspondence detail: hailukendie@gmail.com*

Submitted on: 2025, 3 February; accepted on 2025, 11 July. Section: Research Papers

Abstract: In the Amhara region of Ethiopia, severe soil erosion problems have been a persistent issue due to long-term human-related activities, intense rainfall events, and erosion-sensitive landscapes. The regional government initiated a campaign-based soil and water conservation (SWC) program in response to this pressing issue. A comprehensive soil erosion modeling study was conducted to evaluate the effectiveness of these interventions. The findings show the positive impact of implementing community-based watershed management practices for combating erosion in the region. Specifically, the findings revealed a decline in soil loss from 22.67 Mg ha^{-1} yr^{-1} in 2014 to 20.75 Mg ha^{-1} yr^{-1} in 2022, indicating a reduction of 1.92 Mg ha^{-1} yr^{-1}. This decline in soil loss in the region can be directly related to the successful implementation of community-mobilized SWC measures that have been in place since 2011. Despite this progress, it is still alarming to note that a significant 68.61% of the region is classified as high-risk, highlighting the pressing need for immediate action to address soil erosion. Upon examination of the distribution of soil loss across the region, it is evident that cropland, which makes up 39.73% of the total area, is responsible for a substantial 52.04% of the estimated soil loss. Among the 14 agroecology, the warm moist lowlands, tepid sub-moist mid-highlands, and tepid moist mid-highlands cover 48.65% of the total area and contribute a staggering 73.33% of

the overall soil loss, underscoring the need for location-specific conservation efforts in these areas to mitigate further degradation.

Keywords: Agroecology, Amhara region, soil and water conservation, slope class, soil type

Introduction

Soil erosion by water, identified as a serious global problem by Borrelli et al. (2017) and Sartori et al. (2024), poses significant threats to various aspects, including soil health, agricultural productivity, the global economy, siltation of reservoirs, and food security. Soil erosion is projected to threaten up to $625 billion in global economic contraction by 2070, leading to food security issues in areas at risk, such as Africa and tropical regions (Sartori et al., 2024). The detrimental effects of soil erosion could be seen in the reduction of soil fertility, leading to lower crop yields and reduced agricultural productivity (Hurni et al., 2015; Ebabu et al., 2020). Additionally, the siltation of reservoirs due to soil erosion has negative implications for irrigation water resource development projects and hydro-power generation (Lemma et al., 2018; Fenta et al., 2021), ecosystem services, including the disruption of natural habitats and the alteration of ecological dynamics (Kaffas et al., 2022). Additionally, Sartori et al. (2019) documented that soil erosion causes 33.7 million megagrams (Mg) of agricultural and food losses, resulting in an annual monetary loss of $8 billion globally, ultimately the worldwide agri-food prices increase by 0.4% to 3.5% based on the type of food product category.

It is crucial to note that climate change is projected to exacerbate the problem, with an estimated 66% increase in soil erosion in the Global South, particularly in African countries, between 2015 and 2070 (Borrelli et al., 2020). This trend places the Ethiopian highlands, already recognized as some of the most degraded lands in Africa (Fenta et al., 2020; Tamene et al., 2022), under severe threat. The degradation of the Ethiopian highlands is primarily attributed to a combination of factors, including the growing number of human and livestock populations, steep-slope farming, and deforestation (Kassawmar et al., 2018; Berihun et al., 2019; Abiye et al., 2023). These practices have caused considerable damage to the ecology of several highland areas, pushing the ecosystems to a state that is sometimes beyond recovery (Taddese, 2001).

Ethiopia heavily relies on agriculture as a livelihood source, making the decline in productivity caused by land degradation a major obstacle to achieving food security (Hurni et al., 2015). Over 80% of Ethiopians are employed in agriculture, which is the country's primary economic sector and accounts for over 42% of gross domestic product (GDP) (MoFED, 2010; Diao et al., 2010; Gebregziabher et al., 2016). Amhara National Regional State (ANRS) is predominantly an agricultural region, where agriculture heavily dominates the regional economy by employing over 90% of the workforce and contributing about 54% to the GDP (ARBoFED, 2022). However, the development of the agricultural sector in the region is slower compared to the population growth. One of the main causes of this slow growth is soil erosion by water, particularly the severe loss of topsoil due to the lack of proper implementation of integrated community-based watershed management (ICWM) intervention (Addis et al., 2024). Similarly, Desta (2000, 2005) conducted research between 1995 and 2000 and found that the major degradation processes in the region were water-induced soil erosion and vegetation degradation.

Considering the challenges posed by degradation in the Amhara region, there is an opportunity for implementing a more sustainable community-mobilized SWC program (Adgo et al., 2013; Selassie et al., 2015; Addis et al., 2024). This program aims to address land degradation challenges by implementing proven SWC practices, with the participation of the local communities (Agidew & Singh, 2018; Bayle & Muluye, 2023; Addis et al., 2024). Engaging communities in SWC efforts makes it possible to establish a sense of ownership and stewardship towards the land and its natural

resources, leading to more sustainable land management (SLM) practices and improved livelihoods (Nigussie et al., 2017). To enhance the effectiveness of the community-mobilized SWC program, some policy alternatives should be considered (de Graaff et al., 2013). These options include offering financial and technical assistance to farmers to implement conservation measures (de Graaff et al., 2008; Nigussie et al., 2017), promoting the adoption of climate-smart agricultural practices (Diro et al., 2022), encouraging reforestation and afforestation efforts (Zhang et al., 2016), and strengthening institutional capacities for SLM (Musafiri et al., 2022).

Implementing SWC interventions has become essential to transforming degraded lands into established economic and environmental successes (Brooks & Eckman, 1998; Cooper et al., 2008; Hurni et al., 2015). Notable examples are the successful implementation of SWC interventions in the Loess Plateau and the three gorge areas in China, where the efforts have yielded positive outcomes (Zhao et al., 2013; Shi et al., 2004). Similarly, in India, the Mayurakshi, Salaiyur, and Adarsha watersheds have seen significant improvements due to the SWC interventions (Chowdary et al., 2009; Sikka et al., 2002; Wani et al., 2003). Furthermore, the successful transformation of the Merguellil catchment in Tunisia was attributed to the SWC interventions (Lacombe et al., 2008). In Kenya, the successful implementation of SWC interventions in the Machakos district has been documented by Tiffen and Mortimore (1992), Cooper et al. (2008), and FAO (2014). Lastly, in Ethiopia, the Abraha Atsbaha, Enabereid, Maybar, Haro, Debre Mawi, and Tigray northern Ethiopia catchments have all benefited greatly from SWC interventions, as evidenced by the work of Haregeweyn et al. (2012), Tesfaye et al. (2017), and Gebremeskel et al. (2018).

The primary objective of this study was to generate a soil loss severity map at the regional level and evaluate the effectiveness of mass-mobilized community watershed management practices in reducing soil erosion over different periods. With this in mind, our specific goals were (i) to estimate the spatiotemporal pattern of erosion and severity of soil loss by water at the regional level; (ii) to conduct a detailed analysis of soil loss over various agroecological zones, land cover types, soil types, and slope classes; and (iii) delineate areas that are especially prone to erosion and in need of targeted management interventions.

Study area description

Amhara National Regional State (ANRS) is situated in the northwest of Ethiopia. From a geographical perspective, it lies between 95000 E to 1605000 N and 620000 E to 995000 N (Figure 1). It is bounded by the Afar in the east, Benishangul-Gumuz in the southwest, Oromia in the south, Tigray region in the north, and Sudan in the west. The region's total area is estimated at 180,047 km^2 or almost 16% of the country's total area (BoA 2023). The regional average slope gradient is 23.39%, and the mean elevation is 1805.19 m.a.s.l., with elevations varying from 484 m.a.s.l. in Qwara, West Gonder, to 4620 m.a.s.l. at Ras Dejen (Dashen), North Gonder, which is also the country's highest point (Figure 2). The region exhibits significant geographical changes in temperature due to its wide elevation range, closeness to the equator, and proximity to the Indian Ocean.

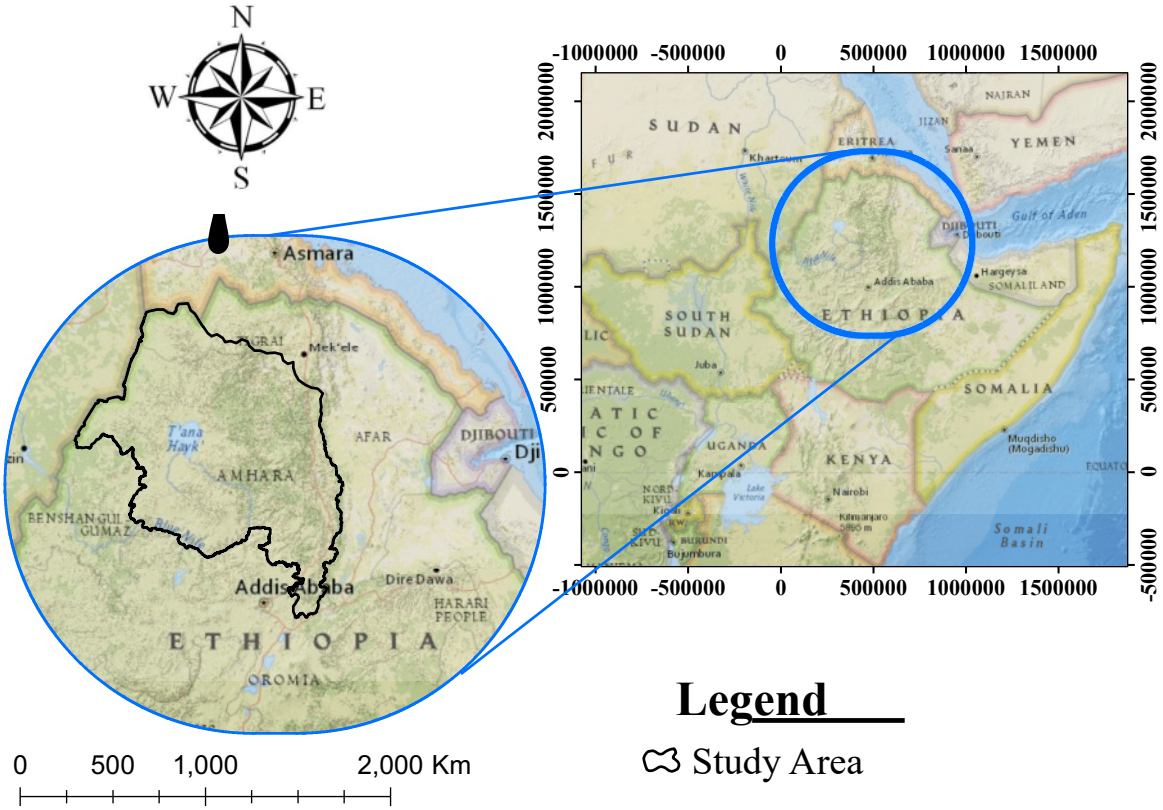

Figure 1. Location map of Amhara region

Highland regions (>1500 m a.s.l.) typically have comparatively colder temperatures than lowland regions (<1500 m a.s.l.). For instance, the mean annual temperature ranges from 21 to 27°C in the hot to warm sub-moist agro-ecological zone, which is located between 600 and 1400 m above sea level, and from 7.5°C to 16°C in the cold to very cold moist zone, which is located between 2800 and 4200 m above sea level (CEDEP 1999). According to the country's primary geomorphic classification, Amhara is composed of seven geomorphic units and four river basins: Abay, Tekeze, Danakil, and Awash. These include the lowlands and scarps in the east, the degraded areas of North Gonder and Wello, the plateaus of Gojam and North Shewa, the Tana plain, the gorges of Abay and Tekeze, the mountainous and afro-alpine regions that include Adama, Amba Farit, Abune Yosef, Guna, Choke, and Ras Dejen (Desta et al., 2000). In addition, the region is the source of large rivers (Abay, Tekeze, Awash, and Golina), and approximately its surface water resource is 75.1 billion cubic meters (BMC) (38.6% of the country) and underground water resources are 5.1 BMC (17% of the country). The potential land that can be irrigated in the region is 1.1 million hectares, but only 20% is being cultivated (BoA, 2023).

The Amhara region is distinguished by its unique topography, which ranges from rugged terrain to flat plains. After dividing the digital elevation model (Figure 2a) into six slope classes (FAO, 2006; Nut et al., 2021); 7.91% of the area is very gently sloping (0–2%), whereas 20.49% and 23.45% of areas are categorized as gently sloping (2–5%) and sloping (5–10%), respectively. The remaining study areas are divided into strongly sloping (10–15%), moderately steep (15–30%), and steep (>30%), which cover areas of 13.57%, 25.43%, and 9.16%, respectively (Figure 2b).

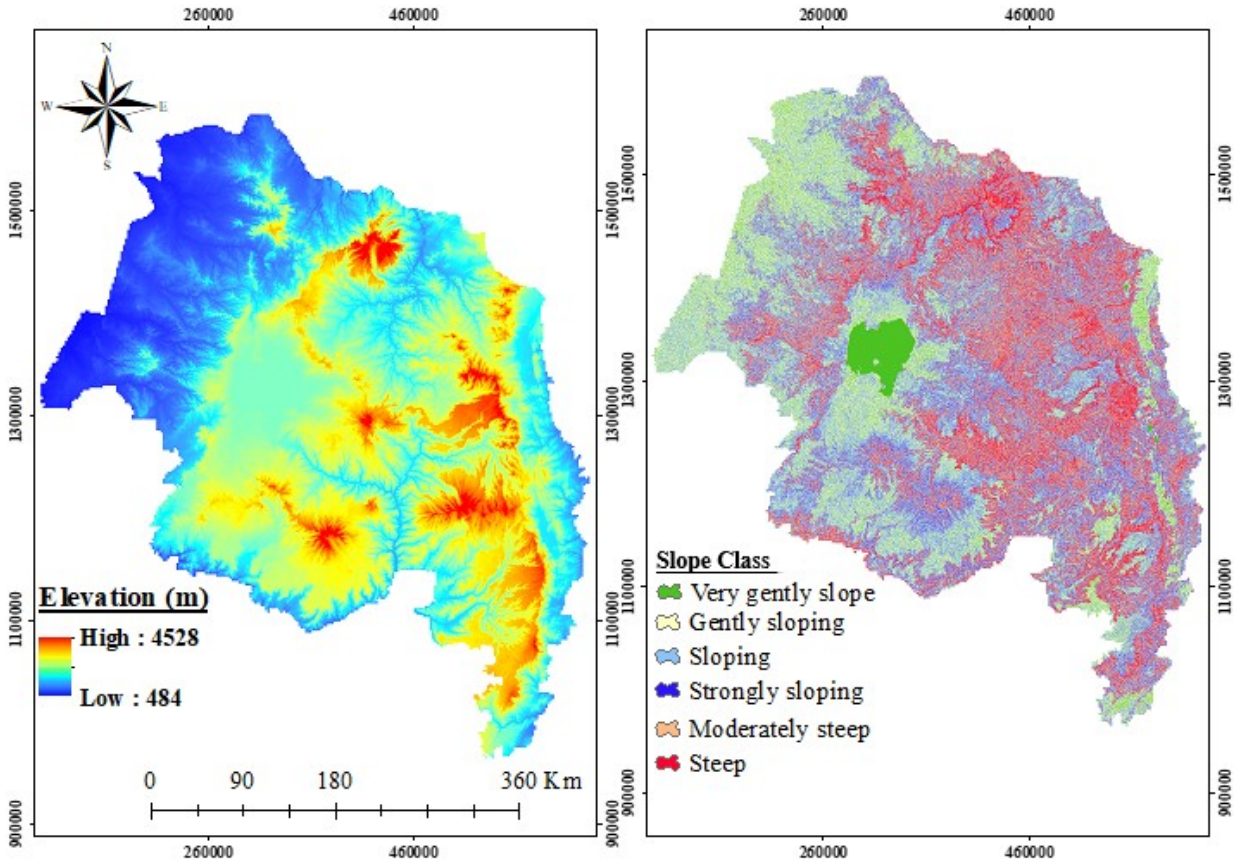

Figure 2. Elevation and slope map of Amhara region

Soil type

According to Wei et al. (2008), soil heterogeneity is a natural occurrence due to different soil-forming factors. Climate, topography, parent material, time, and biological characteristics, including vegetation, land use, and organism activity, are the primary factors that influence soil formation (Regassa et al., 2023). In Amhara region, about 15 soil types have been identified, with a distribution that is very much influenced by the topography and geology of the region. The major soil types occupying more than 90.66% of the study area include Cambisols (35.13%), Vertisols (17.14%), Regosols (14.21%), Luvisols (8.05%), Leptosols. (7.14%), Nitisols (4.18%), Xerosols (4.02%). Other soil types including Fluvisols (2.24%), Solonchacks (2.27%), Gleysols (1.23%), Arenosols (0.85%), Andosols (0.95%), Acrisols (0.40%), Yermosols (0.04%), Phaeozems (0.02%), Histosols (0.003%) also occur in the study area and Open water areas are 1.89% of the total study area (Figure 3).

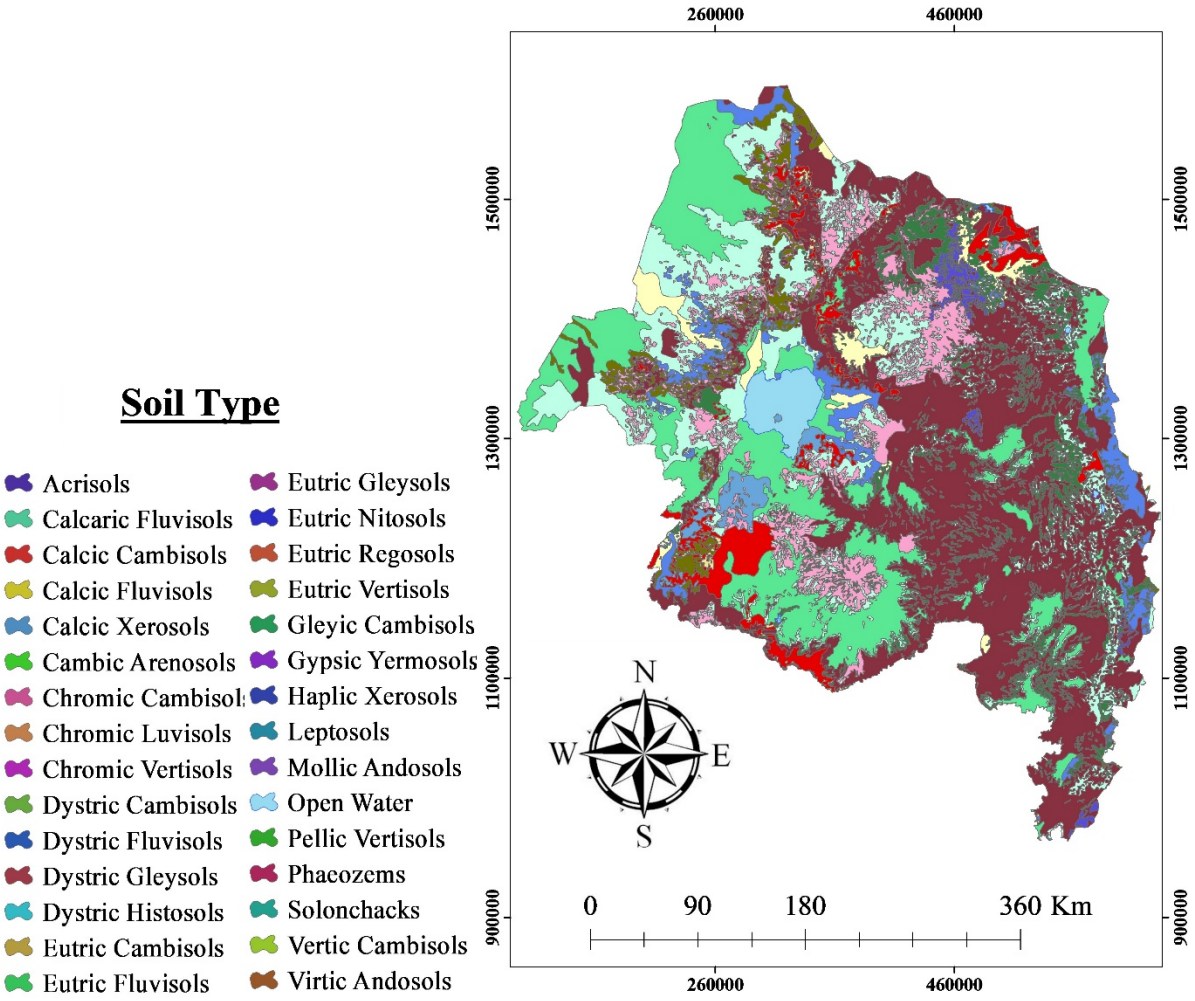

Figure 3. Soil map of Amhara region

Agroecology

Agroecology was initially introduced as an agronomic and technical alternative to traditional agriculture (Wezel et al., 2009). It was thought to replace input intensity with techniques based on biodiversity and knowledge (Altieri & Nicholls, 2012). While helping to achieve the Sustainable Development Goals (SDGs), agroecology helps to preserve biodiversity and restore drylands, which are especially threatened by food insecurity and global warming (Tittonell et al., 2020). Information on temperature and precipitation variance, especially in connection with plant growth requirements, is frequently taken into account in the detailed zonation of agroecology (Patt et al., 2005). The Amhara region is composed of 14 major agroecologies and is dominated (25.95%) by the warm moist lowlands, which has high agricultural potential (Figure 4).

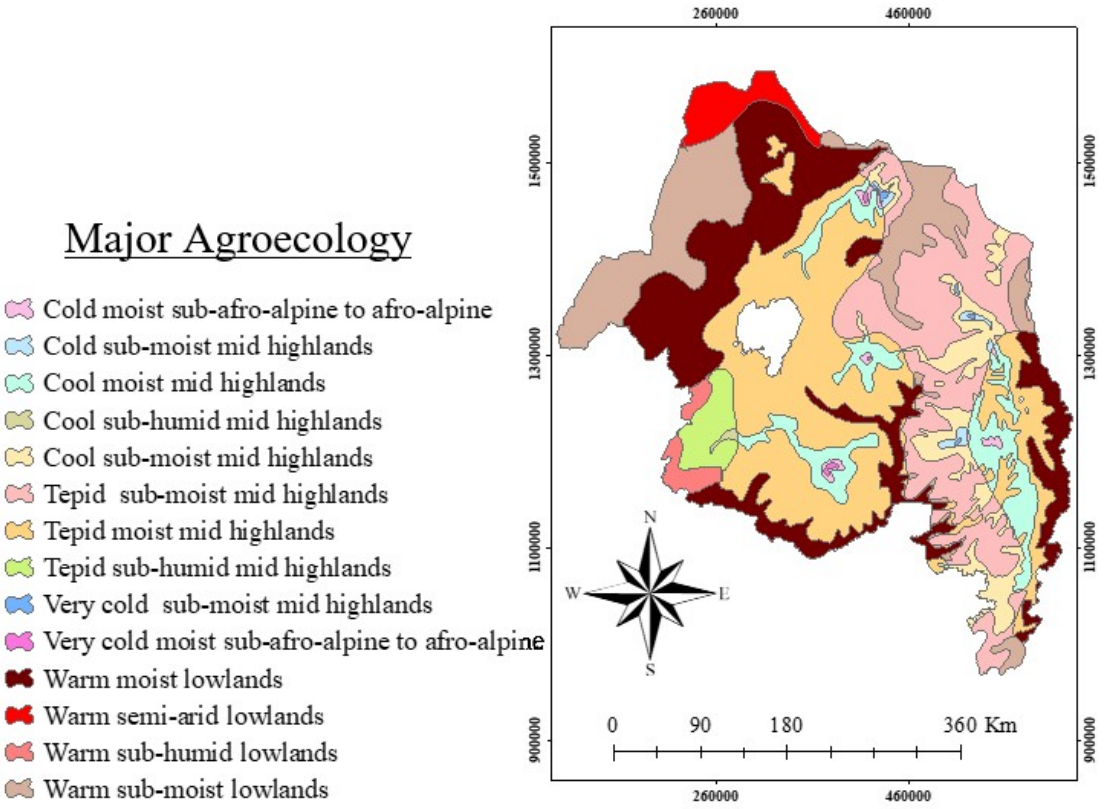

Figure 4. Agroecological map of Amhara region

Climate

The regional average annual rainfall ranges from 378 mm in the east (Habru and Kobo weredas of North Wello and Wag Hemra) to more than 2000 mm in the west (Awi zone), which includes Banja Shikudad, Sekela, and Guangua weredas. With precipitation surpassing 1200 mm annually, the western portions of the region are often classified as having high rainfall and great agricultural potential. The North Wello and Wag Hemra zones in the Amhara region have little rainfall and low agricultural potential. In general, the west and east of the region experience unimodal and bimodal rainfall patterns, respectively. The growing season in the region's western portion ranges from less than 90 days, particularly in the West Gonder zone to over 270 days in Awi zone. In contrast, the region's eastern and southeast parts have growing periods ranging from 45 ─ 90 and 60 ─ 210 days, respectively (BoA 2023).

Land use land cover (LULC)

The way land is utilized, such as agriculture, urban development, or vegetation, directly influences how water flows through the landscape and how sediments are transported (Taye et al., 2013; Betru et al., 2019; Tesfaye et al., 2021). Approximately 30% of the region's total land area, or 4.64 million hectares, is suitable for agriculture; of this, 97% is under cultivation, with 75% of the total area being used for cereal production (BoA, 2023). However, the cultivated land is not very productive (Fenta et al., 2021), primarily due to soil erosion-induced land deterioration (Hurni et al., 2015), inadequate use of modern agricultural technologies (Melaku et al., 2024), and recurrent

and severe droughts (Mera, 2018). Although there is about 1.1 million hectares of irrigation potential in the study area, barely 20% of it is now under cultivation (CoSAERAR 1999). Based on the 10 m resolution European Space Agency WorldCover 2021 Global land cover product (Zanaga et al., 2022), the major land use types in the study area are cropland (39.7%), grassland (27.8%), shrubland (20.6%), forest (8.5%), open water (1.9%), barren (0.9%), built-up (0.4%), and wetland (0.2%) (Figure 5).

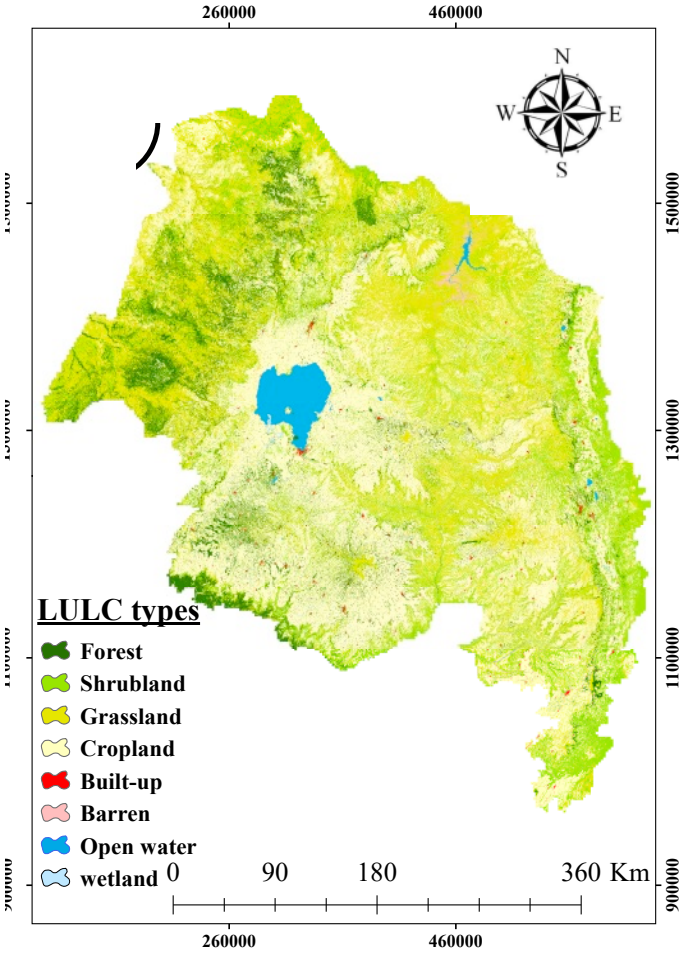

Figure 5. Land use map of Amhara region, source extracted from a 10 m resolution European Space Agency (ESA) World Cover product

Materials and methods

RUSLE model approach

The RUSLE model is crucial for soil erosion estimates, but its accuracy and predictive capabilities are limited by its inability to fully incorporate gully erosion rates, potentially impacting its effectiveness in areas with significant gully erosion. However, in order to determine the best technique, a thorough analysis comparing several RUSLE model approaches was carried out (Table 1). The process of selecting the optimal model involved a thorough evaluation, with a focus on comparing the results and validating our findings with existing research outputs (Shiferaw, 2012; Ayalew & Selassie, 2015; Girmay et al., 2020; Fenta et al., 2021; Tamene et al., 2022). By utilizing

the diverse methodologies (Table 1), the study evaluates the compatibility of each approach in addressing the research output.

Table 1. Approaches and inputs used for the RUSLE model

R-FACTOR	K-FACTOR	LS-FACTOR	C-FACTOR	P-FACTOR
Global erosivity map (Panagos et al., 2017)	DSMW (Sharpley & Williams, 1990)	Moor and Burch (1985)	European Space Agency (ESA) LULC	Shin, 1999
R = -8.12 + 0.562P (Hurni, 1985)		Stone and Hilborn (2012)	ESRI LULC	Wischmeier and Smith (1978)
		Stone and Hilborn (2012) for L-factor and Schmidt et al. (2019) for S-factor	GLOBELAND 30m	
			Sentinel 2 for NDVI (Almagro et al., 2019)	

Note: DSMW = FAO Digital Soil Map of the World; LULC = Land Use Land Cover; Bolded ones were chosen as the best equations for the RUSLE model.

Gathering and processing data for RUSLE model

The annual precipitation, satellite imaging, soil, and terrain data for the years 2014 and 2022 were gathered from several online data repositories, and all the geospatial datasets were then transformed to have a spatial resolution of 30 meters.

Data analysis approach for soil erosion by water

Available soil erosion models extend a spectrum from simple empirical approaches, such as RUSLE (Renard et al., 1997), to complex process-based models, including SWAT (Arnold et al., 1998), EUROSEM (Morgan et al., 1998), and WEPP (Flanagan et al., 2001). Although process-based erosion models require a lot of input data and calibration procedures in order to explain soil loss at fine spatiotemporal scales, their accuracy in predicting soil loss is only slightly better than that of basic empirical erosion models (Tiwari et al., 2000; Jetten et al., 2003). In areas where data is scarce, it is crucial to choose a modeling technique that allows for flexibility in terms of data input, erosion factor modification, and simulation of the possible impact of various management actions on soil loss reduction. The RUSLE model was used because it can estimate soil loss in large spatial domains (Panagos et al., 2015a; Borrelli et al., 2017), has a low computational cost and a modest data demand (Tamene & Le, 2015; Haregeweyn et al., 2017; Fenta et al., 2020), and is compatible with remote sensing data and GIS tools. However, the model does not account for deposition, sediment yield, gully/channel erosion, or landslide (Renard et al., 1997). RUSLE is a user-friendly computer program and a set of mathematical equations that can predict long-term soil loss per year by sheet and rill erosion (Renard et al., 1997). The RUSLE program makes soil loss prediction easier, and it maintains the same basic six-factor structure as the original USLE. Besides, the RUSLE model output allows the user to identify the spatial pattern of the soil loss (Sardari et al., 2019). This feature permits users to identify and categorize locations that are at high risk of

experiencing erosion, either in agricultural fields or wider catchment areas. The following equation (Eq. 1) was used for RUSLE model:

$$A = R * K * L * S * C * P \quad \text{..... (1)}$$

Where; A = estimated mean soil loss per year (Mg ha^{-1} yr^{-1}), R = erosivity factor (MJ mm ha^{-1} h^{-1} yr^{-1}), K reflects soil erodibility factor (Mg h MJ^{-1} mm^{-1}), LS = slope length and gradient factors, dimensionless, C = cover management factor, dimensionless and P = conservation practice factor, dimensionless.

The data source for the runoff erosivity index was the Global Rainfall Erosivity Database (GRED) (Panagos et al., 2017). The data source for the soil erodibility (K) factor was acquired from the Harmonized World Soil Database (HWSD) (Fischer et al., 2008; Nachtergaele et al., 2023). Topographic (LS-factor) data was derived using the Digital Elevation Model (DEM) obtained from the USGS Earth Explorer data portal. This study used Landsat 8 satellite imagery for the year 2014 and Sentinel-2a for the year 2022 to compute the crop management factor (C-factor) and supporting conservation practices (P-factor). Table 2 presents a list of parameters for calculating soil loss using the RUSLE model for the years 2014 and 2022, along with their data sources.

Table 2. A list of parameters and their data sources for estimating soil loss for the years 2014 and 2022

PARAMETERS	DEFINITION	SOURCE	ORIGINAL SPATIAL RESOLUTION	DATE OF ACQUISITION
R (MJ mm ha^{-1} h^{-1} yr^{-1})	Rainfall/Runoff Erosivity Index	https://esdac.jrc.ec.europa.eu/themes/global-rainfall-erosivity	30 arc-seconds (~1 Km)	20 July 2023
K (Mg h MJ^{-1} mm^{-1})	Soil Erosivity Factor	Using the Harmonized World Soil Database (HWSD) (Nachtergaele et al., 2023)	30 arc-seconds (~1 Km)	20 July 2023
LS	Slope and length of Slope Factor	Using DEM from 'USGS's Earth Explorer hub	30 m	20 July 2023
C	Cover Management Factor	Landsat 8 for 2014 ('USGS's Earth Explorer hub) and Sentinel-2a for 2022 (Copernicus open access hub)	30 m (for 2014) and 10m (for 2022)	20 July 2023
P	Supporting Conservation practices	Landsat 8 (for 2014) and Sentinel-2a (for 2022), and slope from DEM ('USGS's Earth Explorer hub)	30 m (for 2014) and 10m (for 2022)	20 July 2023

Estimating rainfall erosivity factor (R-factor)

Rainfall intensity and duration are the main significant factors of the R-factor to cause soil erosion. The most common form of erosion on bare soil surfaces is raindrop/splash erosion, which causes the soil to detach, separate the aggregated soil particles, and initiate their downstream movement

(Arekhi, 2012). The R-factor is computed by multiplying the maximum 30 minutes intensity of rainfall and kinetic energy for individual rainfall events (Wischmeier & Smith, 1978). The cumulative rainfall erosivity factor can also be computed by summing up a series of rainstorm events sampled in the entire study period (Renard et al., 1997). In an ungauged watershed, the R-factor can be calculated using the average annual rainfall data of nearby weather stations (Renard & Freimund, 1994). According to Fenta et al. (2017), the spatial pattern of rainfall erosivity of the study region showed a high degree of correspondence with the global rainfall erosivity (Panagos et al., 2017).

Therefore, for this research, the R-factor was extracted from the Global Rainfall Erosivity Database (GRED) (Panagos et al., 2017). This first-ever GRED was employed to generate a global rainfall erosivity map at a spatial resolution of 30 arc-seconds (~1 km), utilizing Gaussian process regression (Panagos et al., 2017). The output layer map was then transformed to a 30 by 30 m raster grid for the purpose of uniformity with other computation parameters.

Estimating soil erodibility (K-factor)

Erodibility indicates the capability of the soil to withstand detaching, beating, and eroding forces (Getu et al., 2022). Soil's resistance to erosion depends on the topographic position, slope steepness, tillage system, and the properties of the soil, of which the latter is the most significant parameter of soil erodibility (Morgan, 2009). It also depends on the texture of the soil, infiltration capacity, aggregate stability, shear stress/strength, organic matter (OM) content, stone coverage, and clay mineral content. Fine to medium textured soils and soils with low OM content have low infiltration capacity and are more sensitive to water erosion (Lal & Stewart, 1992; Pimentel & Burgess, 2013). The erodibility value designated to a particular soil type reflects the Mg of soil lost per unit of erosive energy compared to bare soil, assuming a standard USLE research plot is 22.1 x 1.83 m, and 9% slope (Renard et al., 1997; Wischmeier & Smith, 1978).

The proportions of sand, silt, clay, and organic carbon (OC) in the topsoil are key determinants in calculating the soil erodibility factor (Wischmeier & Smith, 1978). Although a detailed soil sample is needed to compute the K-factor (Fischer et al., 2008), soil data for this study was obtained from the Harmonized World Soil Database (HWSD) (Mekonnen et al., 2023). HWSD is a raster image linked to an attribute database in Microsoft Access format that includes the determinant soil qualities, such as the topsoil sand, silt, clay, and OC, which are used to calculate the K-factor (Fischer et al., 2008; Nachtergaele et al., 2023). The HWSD raster image layer was extracted by the watershed shapefile using ArcGIS environment, and the attribute data file contained all soil parameters that were joined with the extracted raster layer. The K-factor was then calculated based on the following equations (Eq. 2— 6) developed by Sharpley and Williams, (1990).

$$K = A * B * C * D * 0.1317 \quad \text{..... (2)}$$

Where each letter has its formula:

$$A = \left[0.2 + 0.3 \exp\left(-0.0256 SAN\left(1 - (SIL/100)\right)\right)\right] \quad \text{..... (3)}$$

$$B = \left[\frac{SIL}{CLA+SIL}\right]^{0.3} \quad \text{..... (4)}$$

$$C = [1.0 - (0.25C/\ (C + \exp[(3.72 - 2.95C)]))] \quad \text{..... (5)}$$

$$D = [1.0 - (0.70SN1/(SN1 + \exp[(-5.41 + 22.9SN1)]))] \quad \text{..... (6)}$$

Where: SAN indicates percent sand; SIL indicates percentage of silt and CLA indicates percentage of clay; C indicates organic carbon (OC %) content, and SN1 indicates (1— sand%)/100.

Using ArcGIS format, the final computed K value was added to the attribute table of the masked study area from the soil map, and a raster map was created by clicking the symbology option in properties and then converting it to raster using the attribute value of K-factor to develop a K-factor map. The generated K-factor map was then converted to a 30 x 30 m raster grid.

Estimating slope length and gradient (LS-factor)

Slope steepness accelerates soil loss more quickly than slope length, making slope steepness more important than slope length (Angima et al., 2003). The slope length factor L and the slope steepness factor S, are often lumped together as the topographic factor (LS-factor) (Schmidt et al., 2019). The LS-factor measures the effect of slope length and gradient on soil erosion. When slope length is higher, the opportunity for accumulation and concentration of runoff water is also higher; slope steepness also accelerates the runoff velocity (Brady & Weil, 2008; Wischmeier & Smith, 1978). The 3 arc-sec SRTM DEM with 30 m resolution, retrieved from USGS Earth Explorer (https://earthexplorer.usgs.gov/), was used to calculate the LS-factor. Then, the research area shapefile was used to extract the DEM, and the L and S factors were calculated using raster analysis in ArcGIS. The computation of LS-factor requires pre-processing the slope angle and flow accumulation. The L factor was computed using Stone and Hilborn's (2012) modified RUSLE equations (Eq. 7) as follows:

$$L = (\text{Flow Accumulation} * 30/22.1)^{NN} \quad (7)$$

Where L represents the slope length, determined from the DEM, and NN is a value that depend s on the average slope (Table 3).

Table 3. The NN values based on the average slope

SLOPE	NN
< 1	0.2
1 ≤ s < 3	0.3
3 ≤ s < 5	0.4
> 5	0.5

Originally, the LS-factor was assessed on a 9% steep slope with a length of 22.13 m (Wischmeier & Smith, 1978). The LS-factor is typically restricted to a maximum slope angle of 50% because of its empirical characteristic (McCool et al., 1997; Liu et al., 2015; Schmidt et al., 2019). The Amhara region had a high elevation gradient from 498 m to 4520 m.a.s.l., with a mean elevation of 1805.19 m.a.s.l. and a mean slope gradient of up to 23.39%, a not negligible fraction of slope (13.34%) exceeds the limitation of 50%. To overcome that limitation in LS-factor modeling for steep slope areas, the slope gradient (S) factor was computed based on equation 8 as described by Schmidt et al. (2019).

$$S = (0.0005S\text{^}2 + 0.0795S - 0.4418) \quad (8)$$

Where S indicates the slope gradient factor in percent (%). Then, the L and S factors were multiplied to get the topographic factor (LS-factor) for the RUSLE model.

Estimating cover management factor (C-factor) based on vegetation indices

Normalized Difference Vegetation Index (NDVI)

Normalized difference vegetation index (NDVI) is a simple graphical indicator that is often used to analyze Remote sensing (RS) measurements and determine whether or not the target under observation has green healthy vegetation (Gupta et al., 2021). NDVI values range from +1 to −1, wherein −1 is generally water bodies and +1 is generally dense green–leafy vegetation (Gessesse et al., 2019). Hence, one can say that NDVI is an index to measure healthy green vegetation (Saravanan et al., 2019).

NDVI calculation method

Many researchers have reported the use of NDVI for vegetation monitoring (Carlson & Ripley, 1997; Kinyanjui, 2011; Yang et al., 2011), assessing the crop cover (Lan et al., 2009), drought monitoring (El-Shikha et al., 2007; Wardlow et al., 2007; Kim et al., 2008), and agricultural drought assessment at national (Demirel et al., 2009; Yamaguchi et al., 2010). The vegetation index (VI) is a simple and effective measurement parameter that is used to indicate the Earth's surface vegetation cover and crop growth status in remote sensing fields (Kim et al., 2008). The NDVI analysis for this study was done using two satellite datasets, Landsat 8 (recorded on 20 July 2014) and Sentinel-2a (recorded on 20 July 2022), to determine the rate of changes and ultimately used for computing the C-factor for each year. These periods (2014 and 2022) were selected as the studied area experienced major SWC development programs and land use land cover changes during these periods due to continuous community-mobilized watershed interventions through SWC and an intensive afforestation program. Landsat 8 satellite imagery is downloaded from 'USGS's Earth Explorer hub, for the year 2014, and Sentinel-2a satellite imagery from the (Copernicus open access hub) (Tsendbazar et al., 2018) for the year 2022, then this study calculates the NDVI from red (R) and near-infrared (NIR) band, in the raster calculator, as described by Tucker (1979) (Eq. 9):

$$\mathrm{NDVI} = \frac{(\mathrm{NIR}-\mathrm{R})}{(\mathrm{NIR}+\mathrm{R})} \quad \text{..... (9)}$$

Where NDVI is Normalized Difference Vegetation Index, R is the reflectance of red light (630 nm - 690 nm), and NIR is the reflectance of near-infrared (775 nm - 900 nm).

C-factor calculation method

Soil erosion, runoff generation, and sediment processes taking place within a watershed strongly depend on the land use and land cover types (Welde & Gebremariam, 2017; Anley & Minale, 2024; Argaw & Yohannes, 2024; Mwanga et al., 2024). The RUSLE model provides an estimate of soil loss based on maximum precipitation intensity. Accordingly, this study estimates the C-factor to quantify soil loss during the wettest period of the year in the Amhara region—namely, the late summer monsoon season spanning June to August. Monsoon rainfall consists of localized, often violent thunderstorms, while precipitation during the rest of the year is generally lighter and less significant. In general, higher-elevation and mountainous portions of the region receive more precipitation than lower-elevation areas. In order to identify erosion hotspot areas during the period of annual maximum potential soil erosion, the C-factor is estimated for July, the

peak of the monsoon season. Generating C-factor maps from remotely sensed pictures using vegetation indices like the Normalized Difference Vegetation Index (NDVI) has become a standard procedure (Alexandridis et al., 2015; Feng et al., 2018; Panagos et al., 2015a; Pechanec et al., 2018; Schmidt et al., 2018). The C-factor is determined based on the Normalized Difference Vegetation Index (NDVI) (Almagro et al. 2019), following (Eq. 10):

$$C = 0.1 * (\frac{-NDVI+1}{2}) \quad (10)$$

Support practices factor (P-factor)

The P-factor is the relative proportion of soil loss on certain erosion control practices to the corresponding soil loss if the cultivation system is along the slope (Wischmeier & Smith, 1978). In the RUSLE model, the P value is found to be significantly influenced by the combination of land use types and slope (Behera et al., 2020) and it is among the most challenging factors to determine (Wang & Su 2020) and plays a crucial role in the model's overall accuracy. The influence of SWC on the P-factor is significant yet often overlooked, and this may result in inaccurate estimation of soil erosion potential (Tian et al., 2021). Therefore, a thorough study is necessary to obtain an accurate result of the P-factor. However, because of the unavailability of full data on different control measures in the study area, the land use for the years 2014 and 2022, and the slope gradient from DEM were used as input to calculate and drive the P-factor using Table 4. On the other hand, the spatiotemporal variations in LULC changes between 2014 and 2022 offer valuable insights into the level of community engagement in watershed rehabilitation efforts. By examining how the LULC patterns have changed over these eight years, it becomes possible to determine the level to which local communities have been actively involved in implementing restoration practices. Therefore, the assessment of LULC changes over time not only reveals the landscape dynamics but also offers important insights into the role of community engagement in shaping the future sustainability of the area.

Table 4. Support and management practice (P) value adopted from Wischmeier and Smith (1978)

LULC	SLOPE %	P FACTOR
Crop	0-5	0.1
	5-10	0.12
	10-20	0.14
	20-30	0.19
	30-50	0.25
	50-100	0.33
	>100	1
Non-agricultural land		1

Soil loss estimation and severity mapping

Following the computation and creation of raster layers for the six RUSLE model parameters, the final soil loss estimate was performed by multiplying these values using equation 1 in the raster calculator within the ArcGIS spatial analysis tool. Finally, after predicting total annual soil loss, the erosion severity map was generated by subdividing the study area into 14 agroecological areas, six slope classes, and eight land cover types.

The soil loss severity classification system proposed by Mahapatra et al. (2018) was used. These classes are categorized as very slight (0-2.5), slight (2.5-10), moderate (10-15), moderately severe (15-25), and very severe (25-50) Mg $ha^{-1}yr^{-1}$. However, certain regions within the study area display soil loss exceeding 50 Mg $ha^{-1}yr^{-1}$, prompting the introduction of an additional soil loss class. This new severity class, which was created in this study, takes into account the unique features of the study area and is classified as extremely severe if the rate of soil loss exceeds 50 Mg $ha^{-1}yr^{-1}$.

Results and discussions

RUSLE parameters for soil loss estimation

Using ArcGIS software and the six RUSLE model parameters (rainfall erosivity, soil erodibility, topographic variables, cover management, and erosion control practice factors) annual soil loss was calculated from a cell-by-cell raster calculation. In order to identify areas that require immediate attention and allocate limited resources for erosion control techniques and financial and human resource management, it is crucial to create an erosion severity map (Fayas et al, 2019). This map could also be used as a guide for developmental agents, land managers, and agricultural experts for suitable conservation intervention planning.

Rainfall erosivity (R-factor) estimation

Annual rainfall distribution in the study watershed ranged from 378 to 2156 mm. The computed R-factor using the Global Rainfall Erosivity Database (Panagos et al., 2017) ranged from 1688.67 to 5842.03 MJ mm ha^{-1} h^{-1} yr^{-1} with an average value of 3203.12 MJ mm ha^{-1} h^{-1} yr^{-1} (Figure 6a). Rainfall intensity and duration play a crucial role in determining the R-value. The R-factor carries substantial importance when calculating the total annual soil loss caused by erosion. It holds immense weight in such computations due to the direct correlation between erosivity and erosion. Therefore, protection measures aimed at reducing the detrimental effects of rainfall and runoff can be strategically implemented based on the erosivity values derived from the R-factor.

Soil erodibility (K-factor) estimation

The primary determinants of soil erodibility are the soil organic matter (OM) content and texture (Stone and Hilborn, 2012). Soil with higher OM levels is typically less susceptible to erosion since OM coagulates soil colloids and produces a more stable and aggregated soil structure (Blanco-Canqui et al., 2010). The K-factor value ranges from 0 to 0.6, with low values (0.2 to 0.3) for high water infiltration capacities and moderate soil structural stability, while easily eroded soil has a K-factor of 0.3 or higher (Brady & Weil, 2008).

Based on the HWSD data, the K-factor value for the study area ranged from 0 to 0.126 Mg ha^{-1} MJ^{-1} mm^{-1} with a mean value of 0.056 (Figure 6b). According to the FAO (1984) report, most Ethiopian soil K values range between 0.05 to 0.6, while Getu et al. (2022) stated that the K-factor ranges from 0.1 to 0.49, and the findings of this study also roughly fall within this range.

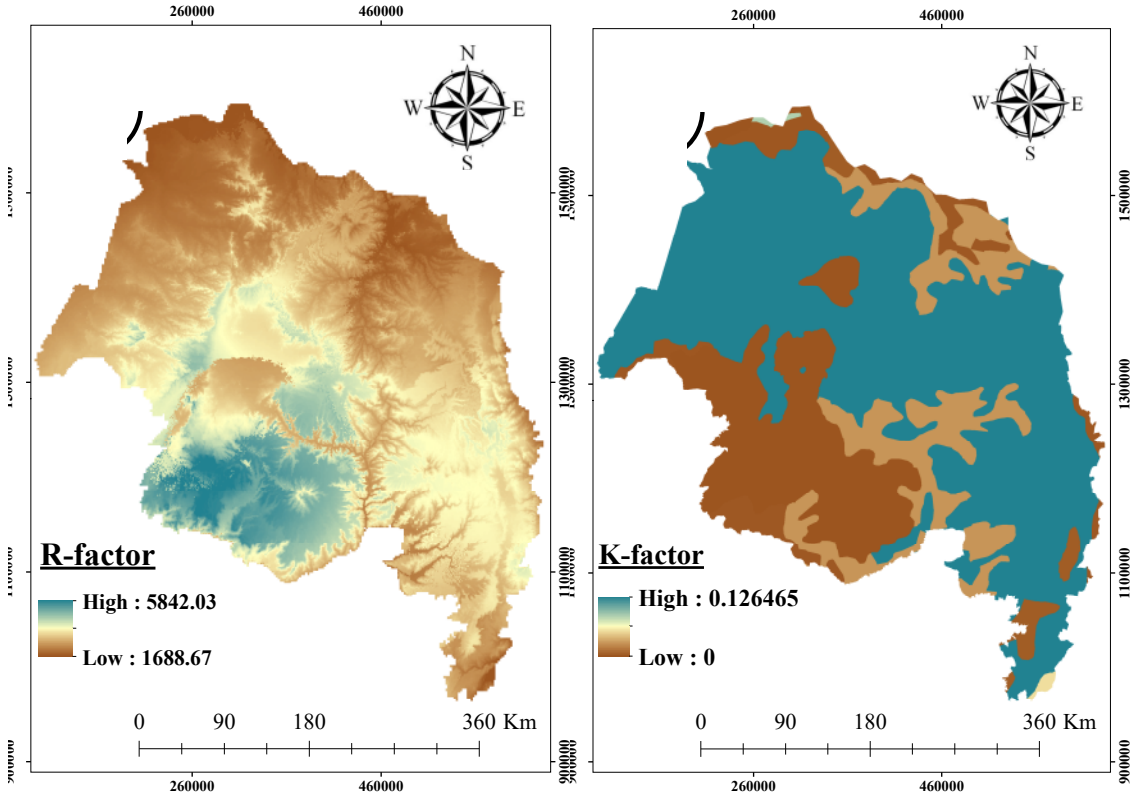

Figure 6. Rainfall erosivity (a) and soil erodibility map (b)

Topographic factor (LS-factor) estimation

The LS-factor is the most predominant factor responsible for soil erosion in the rugged terrain of a mountainous area. Understanding and mitigating the effects of this key factor are essential for sustainable land management practices and conservation efforts in mountainous areas such as those found in the Amhara region. The Amhara region had an extremely steep slope terrain that varied from 0 to 80.45^0 with an average slope of 23.29%. More than 48% of the study area has a slope class greater than strongly sloping ($>10^0$), which exacerbates rill and inter-rill soil erosion (Getu et al., 2022). Based on the results of this research, the LS-factor ranged from 0 to 208.36, with an average value of 4.2 (Figure 7a). The LS-factor is higher in valleys and depressions and increases with elevation gradient and flow accumulation (Schmidt et al., 2019).

Cover management factor (C-factor) prediction

The C-factor was derived by using the NDVI values during the rainy season, considering the erosive rainy period, which contributes to maximum erosion. The NDVI is used along with the equation (Eq. 10) in order to generate a cell-based (30 m X 30 m) annual C-factor map (Figure 7b) of the study area. Results indicate that the C-factor values of the study area ranged from 0.0023 to 0.05, with an average of 0.041.

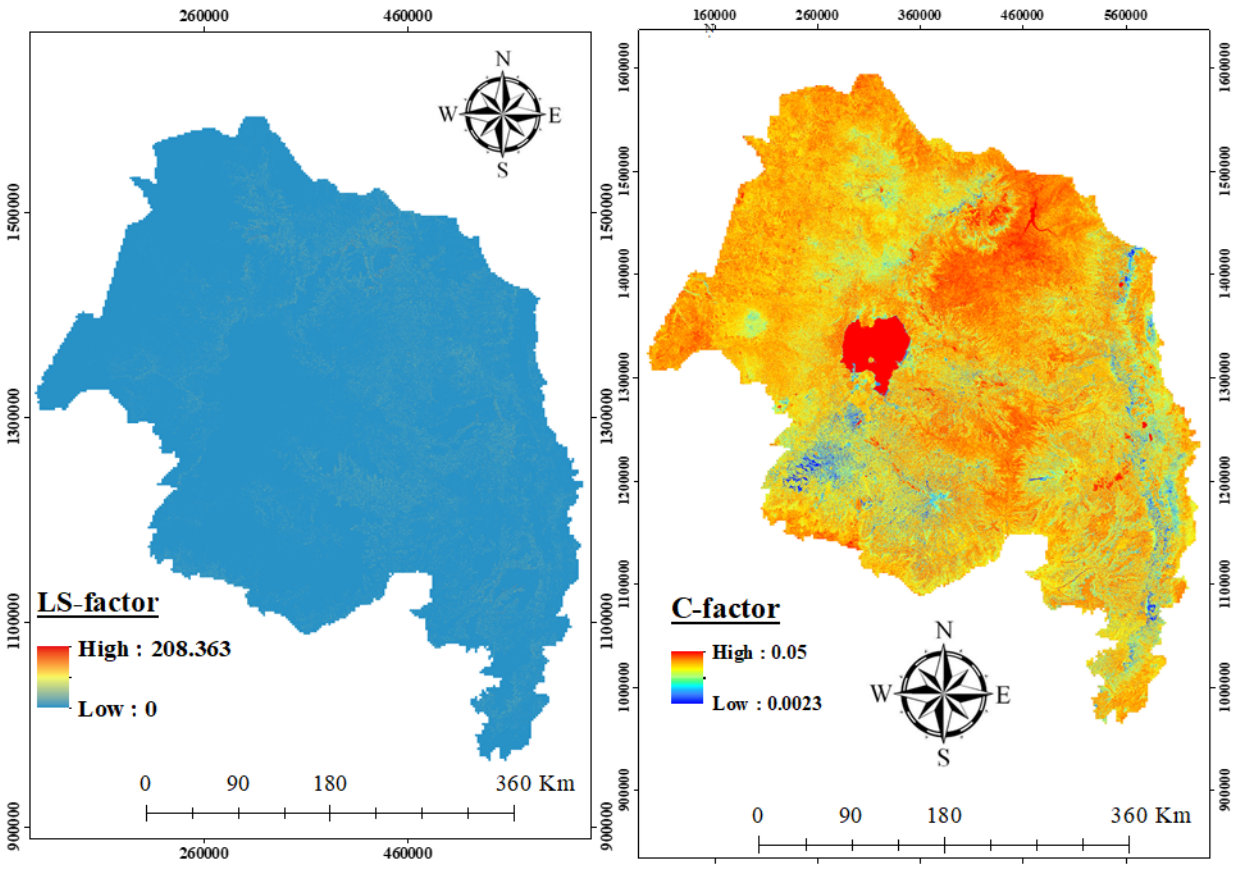

Figure 7. LS-factor (a) and C-factor map (b)

Control practices factor (P-factor) estimation

The combined effect of land use and slope gradient was used as input parameters (Table 4) to calculate and drive the P-factor map (Wischmeier & Smith, 1978). Based on this analysis, the P-factor for the agricultural land ranges from 0.1 to 0.33, while the P-factor value of 1 was assigned for the other landuse types (Figure 8). The spatial patterns of the P-factor map depicted that most of the western and some of the northern parts of Amhara region showed a P value of 1, which indicates that these parts of the region are more prone to soil erosion.

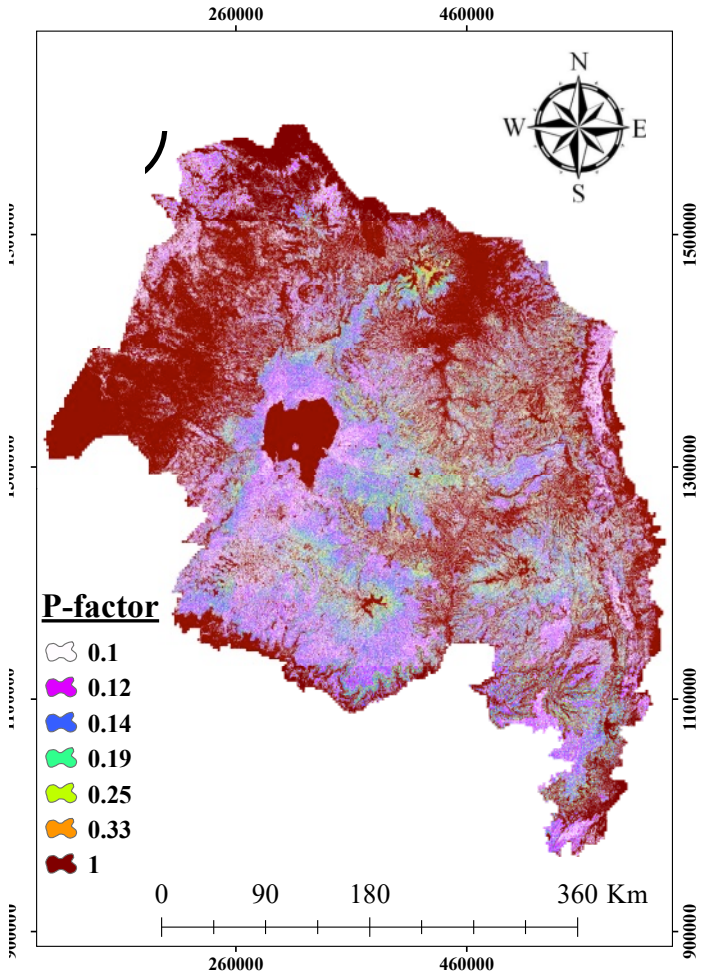

Figure 8. The P-factor map of the region

Estimated soil loss rates and their spatial distribution

The geographical distribution of soil erosion rates in Amara woredas (districts) is shown in Figures 9a and b. According to the figure, the mean soil loss rate in the region during 2022 was 20.75 Mg ha^{-1} yr^{-1}, with a range from 0 to 53.3 Mg ha^{-1} $yr^{-1,}$ and the mean annual gross soil loss was estimated to be 373,597,525 Mg. Upon analyzing the spatial distribution, it was observed that the northern and southeastern highlands of the region experienced highly eroded areas. This erosion was mainly attributed to the high R-factor and LS-factor, as depicted in Figures 6a and 7a, respectively. In contrast, the western Amhara region exhibited lower susceptibility to soil loss from water erosion, likely attributable to reduced C-factor values (Figure 7b). In comparison, areas with gentle slopes (slope <2%) were found to have significantly lower soil loss rates, measured at only 0.001 Mg ha^{-1} yr^{-1}. Despite this, cultivated flat land remains at risk for high soil loss rates, particularly due to the formation of gullies. Such gullies tend to occur on lower slopes where water flow becomes concentrated, as noted by Vanmaercke et al. (2021). This phenomenon poses a significant threat to flat areas that are predominantly used for crop cultivation. Moreover, the activities associated with cropland cultivation can further exacerbate the vulnerability of these areas to soil loss, as highlighted by Fenta et al. (2021).

Meanwhile, comparison with previous studies reveals a range of estimated mean soil loss rates across different areas of the region. For instance, Girmay et al. (2020) estimated the mean soil loss

rates to be 25 Mg ha^{-1} yr^{-1} in the Wag-Himira area, whereas our study revealed a slightly lower estimate of 20.2 Mg ha^{-1} yr^{-1} for this particular region. Similarly, Fenta et al. (2021) estimated a range of 20 to 50 Mg ha^{-1} yr^{-1} for the northeastern area, whereas our findings indicated 25.5 Mg ha^{-1} yr^{-1} in that region. Furthermore, Ayalew and Selassie (2015) estimated the mean soil loss rates to be 24.95 Mg ha^{-1} yr^{-1} in the northwestern parts of the Amhara region, whereas our study revealed a slightly lower estimate of 15.7 Mg ha^{-1} yr^{-1} for that area. The comprehensive research conducted by Tamene et al. (2022) within the tepid sub-moist mid highlands area indicates soil erosion rates that vary from 20.9 to 26.3 Mg ha^{-1}. However, this particular study presented a slightly elevated estimate, documenting an average soil erosion rate of 29.63 Mg ha^{-1} within the same geographical location. Lastly, in South Wollo, Shiferaw (2011) estimated a range of 10 to 80 Mg ha^{-1} yr^{-1} for soil loss rates, whereas our study suggested a specific estimate of 23.6 Mg ha^{-1} yr^{-1} within that region.

The differences in soil loss estimates can be attributed to variations in the models, parameters, and data sources used (Addis et al., 2016), changes in land use (Zhao et al., 2020; Masha et al., 2021; Nigussie et al., 2025), climate (Luvai et al., 2022; Woldemariam et al., 2024), and conservation practices (Alemayehu et al., 2020; Mwanake et al., 2023) variations in local topography (Malleswara Rao et al., 2005), soil types (Ganasri & Ramesh, 2016), and rainfall patterns, which can differ significantly across regions (Woldemariam et al., 2024), and the implementation of soil and water conservation (SWC) measures over time (Alemayehu et al., 2020). These comparisons highlight the variations in soil loss rates within the study area, emphasizing the need for targeted soil conservation measures to mitigate erosion and enhance land productivity.

Variation of soil loss from 2014 to 2022

Soil loss severity in the Amhara region was categorized according to established soil loss severity classes. These categories include very slight, slight, moderate, moderately severe, severe, very severe, and extremely severe, as outlined in Table 5. The soil loss severity classes were determined by the magnitude of soil loss rates, ranging from 1.01 to >51.81 Mg ha^{-1} yr^{-1}. The classification revealed that moderate to extremely severe soil loss severity classes accounted for 68.61% of the total soil loss, while the very slight to slight severity classes accounted for only 31.39%, as indicated in Table 5. Tolerable soil loss (TSL) was first widely used in 1962 when the U.S. Soil Conservation Service proposed TSL values ranging from 4.5 to 11.2 Mg ha^{-1} yr^{-1} for many American soils and defined soil loss tolerance as "the maximum level of soil erosion that will permit a high level of crop productivity to be sustained economically and indefinitely." (Lal, 2001; Di Stefano et al., 2023). This concept was further expanded to include the normal tolerable soil loss (TSL) for Ethiopia, indicating that it ranges from 2 to 18 Mg ha^{-1} yr^{-1} according to the research conducted by Hurni (2015) and Molla and Sisheber (2017). Additionally, studies by Endalew and Biru (2022) and Moges and Bhat (2018) have shown that the TSL for Ethiopia falls within the range of 5 to 11 Mg ha^{-1} y^{-1}, taking into consideration the specific environmental conditions and factors present in the country. Based on those scholars, this finding highlights the urgency of implementing soil and water mitigation measures, as more than two-thirds of the land in Amhara region requires immediate attention to protect against further soil loss, as emphasized by TSL.

According to the RUSLE model, the study area witnessed a significant decrease in soil loss from 22.67 Mg ha^{-1} yr^{-1} in 2014 to 20.75 Mg ha^{-1} yr^{-1} in 2022, representing a reduction of 1.92 Mg ha^{-1} yr^{-1}.

Table 5. Annual average soil loss at each erosion severity class for the 2014 and 2022

SLOPE CLASS %	AREA % 2014	AREA % 2022	AVERAGE SOIL LOSS 2014	AVERAGE SOIL LOSS 2022
Very Slight (0-2.5)	7.76	9.92	1.86	1.70
Slight (2.5-10)	21.80	21.47	5.57	5.82
Moderate (10-15)	12.14	12.23	12.38	13.02
Moderately Severe (15-20)	6.00	8.89	17.82	17.83
Severe (20-25)	13.95	13.36	22.42	22.36
Ver Severe (25-50)	36.20	33.21	36.68	34.42
Extremely Severe (>50)	2.15	0.92	55.67	52.55

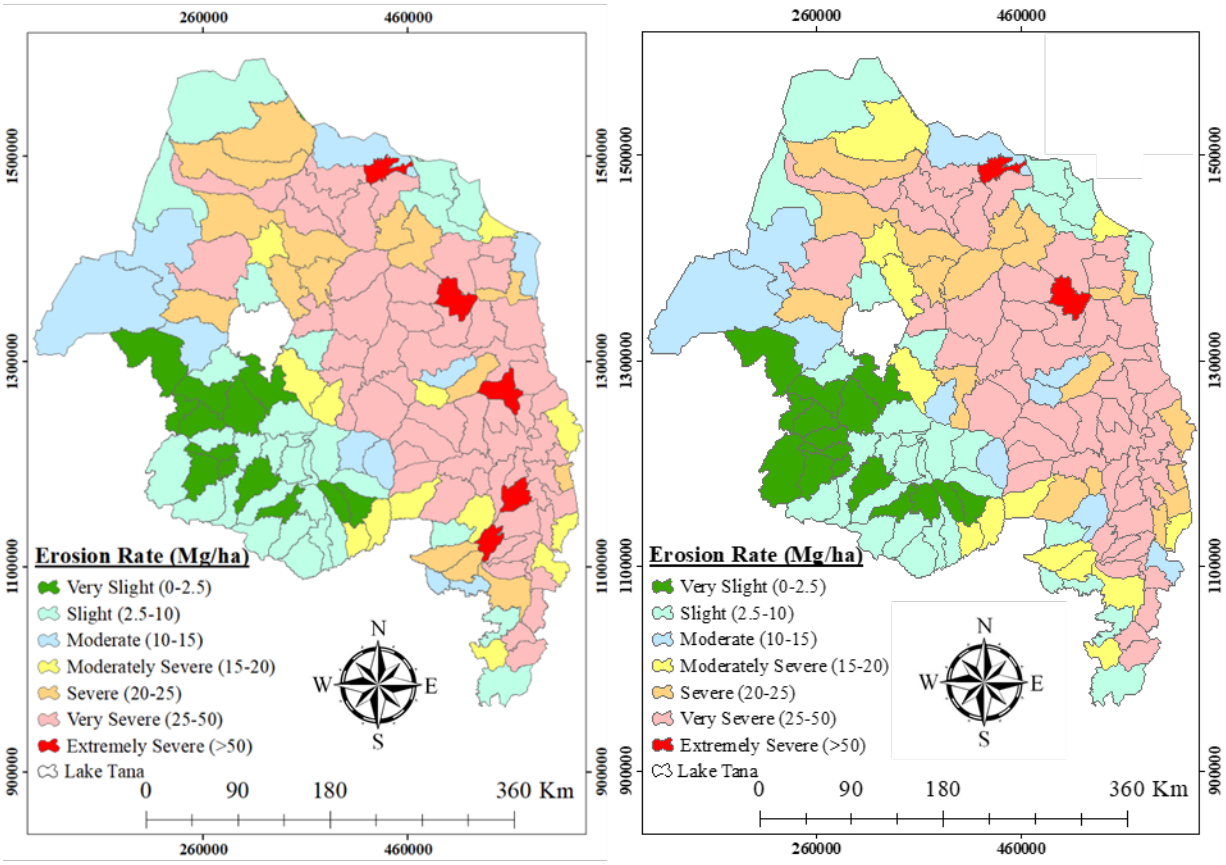

Figure 9. Annual soil loss estimation in each district of Amhara region in 2014 and 2022.

Soil loss estimates by slope class

In the study area, steep slopes (>30%) account for 9.16% of the total land area, yet it is responsible for a significantly high percentage of soil loss. Specifically, in 2014, steep slopes contributed to a staggering 35.75% of the estimated soil loss, and this number increased to 37.99% in 2022 (Table 6). The mean soil loss rate on steep slopes was estimated at 70.16 Mg ha^{-1} yr^{-1} in 2014 and slightly decreased to 67.37 Mg ha^{-1} yr^{-1} in 2022. On the other hand, the remaining slope classes combined contributed 64.25% of the total soil loss in 2014, and this percentage decreased to 62.01% in 2022. This finding further emphasizes the vulnerability of steeper terrains to erosion and highlights the need for effective management strategies in the area. In contrast, very gently

sloping and gently sloping terrains exhibited the lowest soil loss rates of 0.002 and 0.001 Mg ha^{-1} yr^{-1} in 2014 and slightly higher rates of 1.17 and 0.81 Mg ha^{-1} yr^{-1} in 2022, respectively (Table 6). The positive linear relation observed between slope steepness and soil erosion was in conformity with the findings of many researchers (Liu et al., 2000; Jourgholami et al., 2020; Kumar et al., 2023) who also reported linear positive relations on steep slopes.

Table 6. Soil loss estimates for each slope class of the study area for the years 2014 and 2022

Slope class	% of area	Mean soil loss in 2014 (Mg ha^{-1} yr^{-1})	Mean soil loss in 2022 (Mg ha^{-1} yr^{-1})	% of soil loss in 2014	% of soil loss in 2022
Very gently sloping (0–2%)	7.91	0.001933	0.000933	0.00084519	0.000451
Gently sloping (2–5%)	20.49	1.710882	0.80872	1.686099596	0.881949
Sloping (5–10%)	23.45	8.81831	6.815831	9.497975986	8.123563
Strongly sloping (10–15%)	13.57	19.32	16.498272	11.83690811	11.1854
Moderately steep (15–30%)	25.43	36.0049	33.0066	41.2282616	41.8231
Steep (>30%)	9.16	70.164	67.3714	35.74990952	37.98553

Soil loss estimates by land cover types

In the Amhara region, cropland covers 39.73% of the land area, yet it is responsible for a significant 52.04% of the estimated soil loss, according to Table 7. The mean soil loss rate in cropland is 1.5 times that of the overall mean rate, reaching 32.8 Mg ha^{-1} yr^{-1} compared to 20.75 Mg ha^{-1} yr^{-1}. The mean soil loss rate for cropland (32.8 Mg ha^{-1} yr^{-1}) is close to that of 33.3 Mg ha^{-1} yr^{-1} reported by Fenta et al. (2020). On the other hand, shrubland and grassland areas experience mean annual soil loss rates of 20.64 and 27.82 Mg ha^{-1} yr^{-1}, respectively, as indicated in Table 7. Together, these non-cropland covers contribute 40.49% of the total soil loss. In contrast, open water and wetland areas exhibit the lowest soil loss rates at 0.2 and 0.42 Mg ha^{-1} yr^{-1}, respectively. This can be attributed to the low LS-factor and the resultant dense vegetation, as shown in Figures 7a and b. Importantly, cropland contribution to soil loss is approximately 2 to 47 times higher than non-cropland landuse types, proving that converting non-cropland to cropland would further worsen land degradation in the region.

In the study area, cropland stands out as a significant contributor to total soil loss, occupying nearly 39.73% of the regional area and contributing a 52.04% share. Similarly, a study by Fenta et al. (2021) emphasizes that cropland is responsible for approximately 52% of the total soil erosion observed. These results highlight the pivotal role of cropland in soil erosion processes, emphasizing the urgent need for effective land management strategies to mitigate these adverse effects. Meanwhile, shrubland and grassland experience lower soil loss rates (20.64 and 27.82 Mg ha^{1} yr^{1}, respectively) compared to cropland, highlighting the importance of maintaining natural vegetation to reduce erosion, as stated by Nigussie et al. (2025). Hence, a practical approach to mitigating erosion and maintaining soil health involves implementing strategies to limit the expansion of agricultural land. Various research studies, including the works by Shulstad & May (1980), Li et al. (2006), Zhang et al. (2021), and Wang et al. (2024), have underlined the detrimental impact of converting non-cropland areas into cropland. Such conversions not only contribute to the exacerbation of soil erosion but also disrupt the delicate ecological balance of these non-cropland regions (Galindo et al., 2022; Tian et al., 2023).

Table 7. Annual soil loss at each land use/land cover type for the 2022

LAND COVER TYPE	AREA (KM^2)	% OF LULC AREA	MEAN SOIL LOSS ($MG\ HA^{-1}\ YR^{-1}$)	% OF SOIL LOSS
Cropland	71532.67	39.73	32.8	52.04
Built-up	648.17	0.36	38.6	0.55
Barren	1602.42	0.89	35.95	1.28
Forest	15340.00	8.52	16.51	5.62
Shrubland	37161.70	20.64	19.67	16.21
Grassland	50089.08	27.82	21.85	24.28
Open water	3402.89	1.89	0.2	0.02
Wetland	288.08	0.16	0.42	0.00

Soil loss estimates by agroecology

Among the 14 agroecological zones in the Amhara region (Table 8), the warm moist lowlands, tepid sub-moist mid-highlands, and tepid moist mid-highlands agroecological zones constitute a significant portion, approximately 48.65% of the total area. Interestingly, these zones contribute a staggering 73.33% of the overall soil loss, this could be because of increasing human and livestock populations, continued farming, deforestation, and overgrazing. Within this group, the tepid moist mid-highlands zone holds the highest contribution, amounting to 25.4%, primarily due to its dominance in cropland with a high soil loss rate. It is also important to highlight that the warm moist lowlands, tepid sub-moist mid-highlands, and tepid moist mid-highlands agroecological zones occupy 25.95%, 13.83%, and 8.87% of the total area and contribute 22.42%, 25.75%, and 25.06% of the total soil loss, respectively. In comparison to their area coverage, other agroecological zones like the cool sub-humid mid-highlands, warm semi-arid lowlands, warm sub-humid lowlands, and tepid sub-humid mid-highlands have a lower contribution to the total soil loss. This is mainly attributed to their low LS-factor as depicted in Figure 7a. The very cold sub-moist mid highlands cover only 0.03% of the total area but exhibit the highest mean soil loss of 56.46 Mg ha-1 yr-1 in 2022 (Table 8). This result further emphasizes the importance of considering the different agroecological zones when addressing soil erosion issues in the Amhara region. The study conducted by Fenta et al. (2021) also describes the significance of this factor for guiding effective and sustainable solutions in soil conservation practices to combat soil erosion.

Table 8. The major agroecology with area coverage, mean rates of soil loss by water, and percent of total soil loss in Amhara region.

Major Agroecology	Area (Km^2)	% of total area	Soil loss (Mg/ha) 2014	% of total soil loss 2014	Soil loss (Mg/ha) 2022	% of total soil loss 2022
Warm moist lowlands	171097.758	25.9466	21.24	22.42	19.61	22.86
Tepid moist mid highlands	91168.569	13.82551	20.42	25.72	18.26	25.40
Cool moist mid highlands	19631.093	2.977012	28.49	8.57	24.88	8.26
Cold moist sub-afro-alpine to afro-alpine	788.294	0.119543	30.92	0.66	29.02	0.69
Very cold moist sub-afro-alpine to afro-alpine	152.461	0.02312	22.48	0.11	21.79	0.12
Warm semi-arid lowlands	31132.098	4.721114	2.28	0.33	2.19	0.35
Warm sub-humid lowlands	80559.229	12.21663	2.88	0.19	2.69	0.20
Tepid sub-humid mid highlands	75058.374	11.38244	2.00	0.21	1.62	0.18
Cool sub-humid mid highlands	5890.485	0.893279	3.60	0.02	2.63	0.01
Warm sub-moist lowlands	108918.802	16.5173	9.28	7.17	8.83	7.54
Tepid sub-moist mid highlands	58523.571	8.874971	32.71	25.06	29.63	25.07
Cool sub-moist mid highlands	13141.563	1.992889	32.06	8.20	28.16	7.95
Cold sub-moist mid highlands	768.188	0.116494	48.90	1.02	44.72	1.03
Very cold sub-moist mid highlands	180.213	0.027329	60.06	0.33	56.46	0.34
Lake Tana	2,412	0.365774	n.a.			

Note: n.a = not addressed

Soil loss estimates by soil type

The spatiotemporal distribution of soil erosion results in different soil types are presented in Table 9. The soil type that experiences extremely severe soil erosion is Leptosols, experiences extremely severe erosion, covering 7.14% of the total area. In 2014, the mean soil loss for Leptosols was estimated at 60.63 Mg ha^{-1} yr^{-1}, which slightly decreased to 54.62 Mg ha^{-1} yr^{-1} in 2022. Conversely, Cambisols, the dominant soil type in the region, cover an extensive area of 35.13% and contribute to approximately 44.87% of the total soil loss in 2014, which declined slightly to 44.73% in 2022 (Table 9). On average, Cambisols experienced a soil loss of 38.98 Mg ha^{-1} yr^{-1} in 2014 and 36.19 Mg ha^{-1} yr^{-1} in 2022. This could be due to the Cambisol's poor aggregate stability and low permeability to water (Aquino et al., 2013; Heyder et al., 2023) and high erodibility (Tessema et al., 2020), which make this soil more susceptible to erosion.

In 2014, very severe erosion covered the largest area, followed by extremely severe erosion, accounting for 71.69% and 14.18%, respectively. Over the period from 2014–2022, the average value of very severe erosion was dominant, followed by extremely severe erosion, accounting for 69.82% and 13.95%, respectively. Generally, the total areas of very severe and extremely severe erosion were dominant, accounting for 85.88% in 2014 and 81.67% in 2022. This suggests that the situation of erosion in Amhara region has slightly declined over the past decade, and this could be the result of the implementation of SWC interventions and the enhancement of vegetation coverage. Similarly, SWC practices, as highlighted in the study by Mwanake et al. (2023), play a crucial role in preventing soil erosion. Additionally, vegetation cover improvement, as discussed in the studies by Zhao et al. (2020) and Masha et al. (2021), also contributes significantly to reducing soil erosion.

Table 9. Annual soil loss at each soil type in Amhara region

Soil type	Percentage of total area	Soil loss (Mg/ha) 2014	% of total soil loss 2014	Soil loss (Mg/ha) 2022	% of total soil loss 2022	Erosion Rate for 2022
Leptosols	7.14	60.63	14.18	54.62	13.72	Extremely Severe
Regosols	14.21	26.66	12.41	25.42	12.71	Very Severe
Solonchacks	2.27	9.36	0.70	9.23	0.74	Slight
Nitosols	4.18	16.32	2.24	15.07	2.22	Moderately Severe
Acrisols	0.4	40.19	0.53	39.92	0.56	Very Severe
Open Water	1.89	0.25	0.02	0.21	0.01	Very Slight
Arenosols	0.85	26.54	0.74	24.96	0.75	Severe
Yermosols	0.04	5.81	0.01	4.95	0.01	Slight
Luvisols	8.05	36.74	9.69	35.16	9.96	Very Severe
Histosols	0.003	22.91	0.00	18.22	0.00	Moderately Severe
Xerosols	4.02	26.12	3.44	24.60	3.48	Severe
Cambisols	35.13	38.98	44.87	36.19	44.73	Very Severe
Vertisols	17.14	16.61	9.33	15.73	9.48	Moderately Severe
Gleysols	1.23	6.50	0.26	3.94	0.17	Slight
Phaeozems	0.02	26.92	0.02	24.78	0.02	Severe
Fluvisols	2.477	16.09	1.31	14.80	1.29	Moderate
Andosols	0.95	8.73	0.27	5.00	0.17	Slight

Effectiveness of Conservation Measures

Since 2011, community mobilization efforts in the Amhara region lead by the regional government have been successful, with 4 million participants contributing 8 hours a day for 20-30 days annually in the form of free labor, demonstrating their commitment and willingness in a campaign-based SWC intervention for sustainable land management practices (BoA, 2023; Addis et al., 2024). These SWC measures encompassed 128,726.28 hectares of gully rehabilitation, indicating efforts to restore degraded land and prevent erosion in vulnerable areas. Moreover, a vast expanse of 4,436,096.3033 hectares of cultivated fields received SWC measures, indicating a focus on preserving the productivity of agricultural lands. Additionally, 817,104.7 hectares of communal land in the study area were also subjected to SWC interventions (Addis et al., 2024). This highlights the collaborative efforts of the local community in safeguarding their shared resources. Moreover, approximately 7,849.1 hectares were stabilized through bench terracing, while 128,726.28 hectares underwent gully rehabilitation using check-dams—both key soil conservation strategies that contributed significantly to reducing soil loss (Addis et al., 2024). This community-driven approach has been crucial in reducing soil erosion and promoting sustainable land management (SLM) practices. Particularly, the implementation of SWC measures contributed to a significant reduction in soil loss, representing a reduction of 1.92 Mg ha^{-1} yr^{-1}. Therefore, this study highlights the collaborative efforts of local communities in implementing SWC measures to reduce degradation, particularly in communal lands, as stated by Siraw et al. (2018). Extensive physical soil and water conservation (SWC) structures have played a vital role in reducing soil loss and advancing SLM practices, as evidenced by studies conducted by Nyesheja et al. (2019), Kebede et al. (2021), and Kayode et al. (2025).

Management Implications

Annual soil loss estimates for each district in 2014 and 2022 (Figure 9) formed a source of the regional government's environmental monitoring framework. These estimates offered critical insights into spatial variations in soil erosion rates, enabling the identification of districts most susceptible to soil erosion. The temporal comparison between 2014 and 2022 allowed development agents to evaluate trends and measure the effectiveness of conservation interventions over time, as stated by Maximus (2025). This map served as a vital resource for informing policymakers, refining land management strategies, and designing targeted measures to curb soil erosion and improve ecosystem services. The adoption of community-driven approaches, mainly the implementation of soil and water conservation (SWC) measures between 2014 and 2022, led to a measurable reduction in erosion, amounting to a decline of 1.92 Mg ha^{1} yr^{1}.

Meanwhile, 68.61% of the study area experienced moderate to extremely severe soil loss, underlining the urgency for immediate remedial actions. Steep slopes exceeding 30% accounted for 37.99% of total soil loss in 2022, emphasizing the importance of implementing slope-specific conservation approaches, as indicated by Nyesheja et al. (2019). Furthermore, agroecological zones—including warm moist lowlands, tepid sub-moist mid-highlands, and tepid moist mid-highlands—collectively contributed approximately 75% of the total soil loss, despite comprising only half of the study area. In general, the study emphasizes the need

for targeted conservation efforts, particularly in areas with steep slopes, high rainfall erosivity, and vulnerable soil types, as stated by Arega et al. (2024). This aligns with the conclusions of Fenta et al. (2021), who similarly highlight the role of these factors in shaping effective and sustainable soil conservation practices.

Conclusions

This in-depth study was carried out specifically in the Amhara region of Ethiopia, a well-known area that plays a crucial role in sustainable community-mobilized SWC interventions. The main objective is to estimate the effectiveness of campaign-based community watershed management practices in reducing soil erosion over different periods using the RUSLE model. The study showed that the average annual soil erosion rate in Amhara region was approximately 20.75 Mg ha^{-1} yr^{-1}, meaning that 3,157,345,527 Mg yr^{-1} of soil had been lost by 2022. As a result of ICWM interventions, there was a noticeable decrease in soil loss from 22.67 Mg ha^{-1} yr^{-1} in 2014 to 20.75 Mg ha^{-1} yr^{-1} in 2022. The adoption of community-mobilized SWC measures since 2011 is responsible for this decline. However, it is concerning that 68.61% of the region falls into high-risk categories, emphasizing the urgent need for immediate implementation of conservation measures. Analyzing the distribution of soil loss across the region, it is evident that the cropland, which covers 39.73% of the land area, is responsible for a significant 52.04% of the estimated soil loss. Among the 14 agroecological zones in the Amhara region, the warm moist lowlands, tepid sub-moist mid-highlands, and tepid moist mid-highlands agroecological zones stand out, accounting for approximately 48.65% of the total area. Astonishingly, these zones also contribute a staggering 73.33% of the overall soil loss. Therefore, it becomes crucial to utilize severity mapping to identify specific areas requiring targeted conservation practices and investments to combat soil erosion across the entire study area. Understanding the spatial pattern of erosion severity can facilitate the allocation of resources and monitoring of progress on a regional scale, enabling comprehensive and sustainable management of the Amhara region. Therefore, through the implementation of a community-mobilized SWC program, coupled with appropriate policy measures, it is possible to reverse the trend of land degradation and promote sustainable land management practices in Amhara region. This will not only contribute to protecting the environment and natural resources in the region but also improve the livelihoods of the local communities who heavily rely on conventional agriculture.

References

Abiye, W., Waltner, I., & Kindie, H. (2023). Spatiotemporal dynamics of soil erosion response to land use land cover dynamics and climate variability in Maybar watershed, Awash basin, Ethiopia. *Geology, Ecology, and Landscapes*, 1-23.

Addis, H. K., Strohmeier, S., Ziadat, F., Melaku, N. D., & Klik, A. (2016). Modeling streamflow and sediment using SWAT in Ethiopian Highlands. *International Journal of Agricultural and Biological Engineering*, *9*(5), 51-66.

Addis, H. K., Tamir, S., Belay, B., Mekuriaw, S., Birehanu, T., & Wuletaw, Y. (2024). Community-mobilized soil and water conservation and farmers' preferences for mitigating land degradation. *Environmental Research Communications*.

Adgo, E., Teshome, A., & Mati, B. (2013). Impacts of long-term soil and water conservation on agricultural productivity: The case of Anjenie watershed, Ethiopia. *Agricultural Water Management*, *117*, 55-61.

Agidew, A. M. A., & Singh, K. N. (2018). Factors affecting farmers' participation in watershed management programs in the Northeastern highlands of Ethiopia: A case study in the Teleyayen sub-watershed. *Ecological Processes*, 7(1), 1–15. https://doi.org/10.1186/s13717-018-0128-6

Alemayehu, A. A., Muluneh, A., Moges, A., & Kendie, H. (2020). Estimation of sediment yield and effectiveness of level stone bunds to reduce sediment loss in the Gumara-Maksegnit watershed, Nile Basin, Ethiopia. *Journal of Soils and Sediments*, *20*, 3756-3768.

Alexandridis, T. K., Sotiropoulou, A. M., Bilas, G., Karapetsas, N., & Silleos, N. G. (2015). The effects of seasonality in estimating the C-factor of soil erosion studies. *Land Degradation & Development*, *26*(6), 596-603.

Almagro, A., Thomé, T. C., Colman, C. B., Pereira, R. B., Junior, J. M., Rodrigues, D. B. B., & Oliveira, P. T. S. (2019). Improving cover and management factor (C-factor) estimation using remote sensing approaches for tropical regions. *International Soil and Water Conservation Research*, *7*(4), 325-334.

Altieri, M. A., & Nicholls, C. I. (2012). Agroecology scaling up for food sovereignty and resiliency. *Sustainable Agriculture Reviews: Volume 11*, 1-29.

Angima, S. D., Stott, D. E., O'neill, M. K., Ong, C. K., & Weesies, G. A. (2003). Soil erosion prediction using RUSLE for central Kenyan highland conditions. *Agriculture, ecosystems & environment*, *97*(1-3), 295-308.

Anley, M. A., & Minale, A. S. (2024). Modeling the impact of land use land cover change on the estimation of soil loss and sediment export using InVEST model at the Rib watershed of Upper Blue Nile Basin, Ethiopia. *Remote Sensing Applications: Society and Environment*, 101177.

Aquino, R. F., Silva, M. L. N., Freitas, D. A. F. D., Curi, N., & Avanzi, J. C. (2013). Soil losses from typic Cambisols and Red Latosol as related to three erosive rainfall patterns. *Revista Brasileira de Ciência do Solo*, *37*, 213-220.

ARBoFED (Amhara Region Bureau of Finance and Economic Development) (2022). *Annual report*. Bahir Dar, Ethiopia: Bureau of Finance and Economic Development (BoFED).

Arekhi, S., Niazi, Y., & Kalteh, A. M. (2012). Soil erosion and sediment yield modeling using RS and GIS techniques: a case study, Iran. *Arabian Journal of Geosciences*, *5*(2), 285.

Arega, E., Deribew, K. T., Moisa, M. B., & Gemeda, D. O. (2024). Assessment of soil erosion and prioritization of conservation and restoration measures using RUSLE and Geospatial techniques: the case of upper Bilate watershed. *Geomatics, Natural Hazards and Risk*, *15*(1), 2336016.

Argaw, M., & Yohannes, H. (2024). Impact of land use/land cover changes on surface water and soil-sediment export in the urbanized Akaki River catchment, Awash Basin, Ethiopia. *Journal of Hydrology: Regional Studies*, *52*, 101677.

Arnold, J. G., Srinivasan, R., Muttiah, R. S., & Williams, J. R. (1998). Large area hydrologic modeling and assessment part I: model development 1. *JAWRA Journal of the American Water Resources Association*, *34*(1), 73-89.

Ayalew, G., & Selassie, Y. G. (2015). Soil loss estimation for soil conservation planning using geographic information system in Guang watershed, Blue Nile basin. *J Environ Earth Sci*, *5*(1), 126-134.

Bayle, D., & Muluye, K. (2023). Review on successful soil conservation methods in Ethiopia. *Cogent Food & Agriculture*, *9*(2), 2274171.

Behera, M., Sena, D. R., Mandal, U., Kashyap, P. S., & Dash, S. S. (2020). Integrated GIS-based RUSLE approach for quantification of potential soil erosion under future climate change scenarios. *Environmental Monitoring and Assessment*, *192*(11), 733.

Berihun, M. L., Tsunekawa, A., Haregeweyn, N., Meshesha, D. T., Adgo, E., Tsubo, M., ... & Yibeltal, M. (2019). Exploring land use/land cover changes, drivers and their implications in contrasting agro-ecological environments of Ethiopia. *Land use policy*, *87*, 104052.

Betru, T., Tolera, M., Sahle, K., & Kassa, H. (2019). Trends and drivers of land use/land cover change in Western Ethiopia. *Applied Geography*, *104*, 83-93.

Blanco-Canqui, H., Stone, L. R., & Stahlman, P. W. (2010). Soil response to long-term cropping systems on an Argiustoll in the central Great Plains. *Soil Science Society of America Journal*, *74*(2), 602-611.

BoA (Bureau of Agriculture) (2023). Amhara National Regional State Bureau of Agriculture, Natural resource 2023 Annual report: Wereda level. Bahir Dar, Ethiopia

Borrelli, P., Robinson, D. A., Fleischer, L. R., Lugato, E., Ballabio, C., Alewell, C., ... & Panagos, P. (2017). An assessment of the global impact of 21st century land use change on soil erosion. *Nature communications*, *8*(1), 1-13.

Borrelli, P., Robinson, D. A., Panagos, P., Lugato, E., Yang, J. E., Alewell, C., ... & Ballabio, C. (2020). Land use and climate change impacts on global soil erosion by water (2015-2070). *Proceedings of the National Academy of Sciences*, *117*(36), 21994-22001.

Brady, N. C., & Weil, R. R. (2008). *The nature and properties of soils* (Vol. 13, pp. 662-710). Upper Saddle River, NJ: Prentice Hall.

Brooks, K. N., & Eckman, K. (1998). Global perspective of watershed management. *Land Stewardship in the 21stCentury: The Contributions of Watershed Management*, 11-20.

Carlson, T. N., & Ripley, D. A. (1997). On the relation between NDVI, fractional vegetation cover, and leaf area index. *Remote sensing of Environment*, *62*(3), 241-252.

CEDEP (Consultants for Economic Development and Environmental Protection) (1999). Regional Agricultural Master Plan: Main report. CEDEP, Bahir Dar, Ethiopia. 155 pp.

Chowdary, V. M., Ramakrishnan, D., Srivastava, Y. K., Chandran, V., & Jeyaram, A. (2009). Integrated water resource development plan for sustainable management of Mayurakshi watershed, India using remote sensing and GIS. *Water resources management*, *23*(8), 1581-1602.

Cooper, P. J., Dimes, J., Rao, K. P. C., Shapiro, B., Shiferaw, B., & Twomlow, S. (2008). Coping better with current climatic variability in the rain-fed farming systems of sub-Saharan Africa: An essential first step in adapting to future climate change?. *Agriculture, ecosystems & environment*, *126*(1-2), 24-35.

CoSAERAR (Commission for Sustainable Agriculture and Environmental Rehabilitation for Amhara Region) (1999). CoSAERAR brochure. CoSAERAR, Bahir Dar, Ethiopia. 12 pp.

De Graaff, J., Amsalu, A., Bodnar, F., Kessler, A., Posthumus, H., & Tenge, A. (2008). Factors influencing adoption and continued use of long-term soil and water

conservation measures in five developing countries. Applied Geography, 28(4), 271-280.

De Graaff, J., Aklilu, A., Ouessar, M., Asins-Velis, S., & Kessler, A. (2013). The development of soil and water conservation policies and practices in five selected countries from 1960 to 2010. *Land Use Policy*, *32*, 165-174.

Demirel, H., Ozcinar, C., & Anbarjafari, G. (2009). Satellite image contrast enhancement using discrete wavelet transform and singular value decomposition. *IEEE Geoscience and remote sensing letters*, *7*(2), 333-337.

Desta, L., Kassie, M., Benin, S., & Pender, J. (2000). *Land degradation and strategies for sustainable development in the Ethiopian highlands, Amhara Region, Socio-economics and Policy Research Working Paper 32.* International Livestock Research Institute, Nairobi, Kenya.

Desta, L., Carucci, V., Wendem-Agenehu, A., & Abebe, Y. (2005). *Community based participatory watershed development: A guideline.* Addis Ababa, Ethiopia: Ministry of Agriculture and Rural Development (MoARD).

Diao, X., Taffesse, A. S., Yu, B., & Pratt, A. N. (2010, November). Economic importance of agriculture for sustainable development and poverty reduction: The case study of Ethiopia. In *Global forum on agriculture* (pp. 29-30). *Policies for Agricultural Development, Poverty Reduction and Food Security*, November 29-30, 2010, Organisation for Economic Co-operation and Development (OECD) Headquarters, Paris, France.

Di Stefano, C., Nicosia, A., Pampalone, V., & Ferro, V. (2023). Soil loss tolerance in the context of the European Green Deal. Heliyon, 9(1).

Diro, S., Tesfaye, A., & Erko, B. (2022). Determinants of adoption of climate-smart agricultural technologies and practices in the coffee-based farming system of Ethiopia. Agriculture & Food Security, 11(1), 1-14.

Ebabu, K., Tsunekawa, A., Haregeweyn, N., Adgo, E., Meshesha, D. T., Aklog, D., ... & Yibeltal, M. (2020). Exploring the variability of soil properties as influenced by land use and management practices: A case study in the Upper Blue Nile basin, Ethiopia. *Soil and Tillage Research*, *200*, 104614.

El-Shikha, D. M., Waller, P., Hunsaker, D., Clarke, T., & Barnes, E. (2007). Ground-based remote sensing for assessing water and nitrogen status of broccoli. *Agricultural water management*, *92*(3), 183-193.

Endalew, T., & Biru, D. (2022). Soil erosion risk and sediment yield assessment with Revised Universal Soil Loss Equation and GIS: The case of Nesha watershed, Southwestern Ethiopia. *Results in Geophysical Sciences*, *12*, 100049.

FAO. (1984). (Food and agriculture organization/United Nations development programme), methodology used in the development of soil loss rate map of the Ethiopian highlands. Field document 5 (Rome: FAO). https://doi.org/10.1016/j.iswcr.2019.01.003

FAO. (2006). Guidelines for Soil Description, 4th ed.; Food and Agriculture Organization of the United Nations: Rome, Italy, ISBN 978-92-5-105521-2.

FAO. (2014). Adapting to climate change through land and water management in Eastern Africa. *Results of Pilot Projects in Ethiopia, Kenya and Tanzania*.

Fayas, C. M., Abeysingha, N. S., Nirmanee, K. G. S., Samaratunga, D., & Mallawatantri, A. (2019). Soil loss estimation using rusle model to prioritize erosion control in KELANI river basin in Sri Lanka. *International Soil and Water Conservation Research*, *7*(2), 130-137.

Feng, Q., Zhao, W., Ding, J., Fang, X., & Zhang, X. (2018). Estimation of the cover and management factor based on stratified coverage and remote sensing indices: A case study in the Loess Plateau of China. *Journal of soils and sediments*, *18*, 775-790.

Fenta, A. A., Yasuda, H., Shimizu, K., & Haregeweyn, N. (2017). Response of streamflow to climate variability and changes in human activities in the semiarid highlands of northern Ethiopia. *Regional Environmental Change*, *17*, 1229-1240.

Fenta, A. A., Tsunekawa, A., Haregeweyn, N., Poesen, J., Tsubo, M., Borrelli, P., ... & Kurosaki, Y. (2020). Land susceptibility to water and wind erosion risks in the East Africa region. *Science of the Total Environment*, *703*, 135016.

Fenta, A. A., Tsunekawa, A., Haregeweyn, N., Tsubo, M., Yasuda, H., Kawai, T., ... & Sultan, D. (2021). Agroecology-based soil erosion assessment for better conservation planning in Ethiopian river basins. *Environmental research*, *195*, 110786.

Fischer, G., Nachtergaele, F., Prieler, S., Van Velthuizen, H. T., Verelst, L., & Wiberg, D. (2008). Global agro-ecological zones assessment for agriculture (GAEZ 2008). *IIASA, Laxenburg, Austria and FAO, Rome, Italy*, *10*.

Flanagan, D. C., Ascough, J. C., Nearing, M. A., & Laflen, J. M. (2001). The water erosion prediction project (WEPP) model. *Landscape erosion and evolution modeling*, 145-199.

Galindo, V., Giraldo, C., Lavelle, P., Armbrecht, I., & Fonte, S. J. (2022). Land use conversion to agriculture impacts biodiversity, erosion control, and key soil properties in an Andean watershed. *Ecosphere*, *13*(3), e3979.

Ganasri, B. P., & Ramesh, H. (2016). Assessment of soil erosion by RUSLE model using remote sensing and GIS-A case study of Nethravathi Basin. *Geoscience Frontiers*, *7*(6), 953-961. https://doi.org/10.1016/j.gsf.2015.10.007.

Gebregziabher, G., Abera, D. A., Gebresamuel, G., Giordano, M., & Langan, S. (2016). *An assessment of integrated watershed management in Ethiopia* (Vol. 170). International Water Management Institute (IWMI).

Gebremeskel, G., Gebremicael, T. G., & Girmay, A. (2018). Economic and environmental rehabilitation through soil and water conservation, the case of Tigray in northern Ethiopia. *Journal of Arid Environments*, *151*, 113-124.

Gessesse, A. A., & Melesse, A. M. (2019). Temporal relationships between time series CHIRPS-rainfall estimation and eMODIS-NDVI satellite images in Amhara Region, Ethiopia. In *Extreme hydrology and climate variability* (pp. 81-92). Elsevier.

Getu, L. A., Nagy, A., & Addis, H. K. (2022). Soil loss estimation and severity mapping using the RUSLE model and GIS in Megech watershed, Ethiopia. *Environmental Challenges*, *8*, 100560.

Girmay, G., Moges, A., & Muluneh, A. (2020). Estimation of soil loss rate using the USLE model for Agewmariayam Watershed, northern Ethiopia. *Agriculture & Food Security*, *9*, 1-12.

Gupta, H., Kaur, L., Asra, M., Avtar, R., & Reddy, C. S. (2021). MODIS NDVI multi-temporal analysis confirms farmer perceptions on seasonality variations affecting apple orchards in Kinnaur, Himachal Pradesh. *Agriculture*, *11*(8), 724.

Haregeweyn, N., Berhe, A., Tsunekawa, A., Tsubo, M., & Meshesha, D. T. (2012). Integrated watershed management as an effective approach to curb land degradation: a case study of the Enabered watershed in northern Ethiopia. *Environmental management*, *50*, 1219-1233.

Haregeweyn, N., Tsunekawa, A., Poesen, J., Tsubo, M., Meshesha, D. T., Fenta, A. A., ... & Adgo, E. (2017). Comprehensive assessment of soil erosion risk for better land use planning in river basins: Case study of the Upper Blue Nile River. *Science of the Total Environment*, *574*, 95-108.

Heyder, S. M., Beza, S. A., & Demissie, S. T. (2023). Optimization of land management measures for soil erosion risk using GIS in agricultural landscape of western Hararghe highlands, Ethiopia. *Scientific African*, *21*, e01853.

Hurni, K., Zeleke, G., Kassie, M., Tegegne, B., Kassawmar, T., Teferi, E., ... & Hurni, H. (2015). Soil degradation and sustainable land management (SLM) in the rainfed agricultural areas of Ethiopia: an assessment of the economic implications. *Report for the economics of land degradation initiative*, *62*.

Jetten, V., Govers, G., & Hessel, R. (2003). Erosion models: quality of spatial predictions. *Hydrological processes*, *17*(5), 887-900.

Jourgholami, M., Karami, S., Tavankar, F., Lo Monaco, A., & Picchio, R. (2020). Effects of slope gradient on runoff and sediment yield on machine-induced compacted soil in temperate forests. *Forests*, *12*(1), 49.

Kaffas, K., Papaioannou, G., Varlas, G., Al Sayah, M. J., Papadopoulos, A., Dimitriou, E., ... & Righetti, M. (2022). Forecasting soil erosion and sediment yields during flash floods: The disastrous case of Mandra, Greece, 2017. *Earth Surface Processes and Landforms*, *47*(7), 1744-1760.

Kassawmar, T., Zeleke, G., Bantider, A., Gessesse, G. D., & Abraha, L. (2018). A synoptic land change assessment of Ethiopia's Rainfed Agricultural Area for evidence-based agricultural ecosystem management. *Heliyon*, *4*(11).

Kayode, J. S., Olufemi, S. D., Bola, A., Samuel, A. A., Obinna, S. C. (2025). Geospatial analysis of soil erosion and implications for sustainable development goals in tropical ecological zones. *Discov Environ*, 3, 14 (2025). https://doi.org/10.1007/s44274-025-00198-7

Kebede, B., Tsunekawa, A., Haregeweyn, N., Adgo, E., Ebabu, K., Meshesha, D. T., ... & Fenta, A. A. (2021). Determining C-and P-factors of RUSLE for different land uses and management practices across agro-ecologies: case studies from the Upper Blue Nile basin, Ethiopia. *Physical Geography*, *42*(2), 160-182.

Kefale Munye, G. S., Belayneh, A., & Ayalew, M. (2024). Identifying Soil Erosion Hotspot Areas Using GIS and MCDA Techniques: Case. *Land and Water Degradation in Ethiopia: Climate and Land Use Change Implications*, 111.

Kim, H., Kwak, H. S., & Yoo, J. S. (2008). Improved clustering algorithm for change detection in remote sensing. *International journal of digital content technology and its applications*, *2*(2), 55-59.

Kinyanjui, M. J. (2011). NDVI-based vegetation monitoring in Mau forest complex, Kenya. *African Journal of Ecology*, *49*(2), 165-174.

Kumar, G., Kurothe, R. S., Viswakarma, A. K., Mandal, D., Sena, D. R., Mandal, U., ... & Dinesh, D. (2023). Assessment of soil vulnerability to erosion in different land surface configurations and management practices under semi-arid monsoon climate. *Soil and Tillage Research*, *230*, 105698.

Lacombe, G., Cappelaere, B., & Leduc, C. (2008). Hydrological impact of water and soil conservation works in the Merguellil catchment of central Tunisia. *Journal of Hydrology*, *359*(3-4), 210-224.

Lal, R., & Stewart, B. A. (1992). Need for land restoration. *Soil Restoration: Soil Restoration Volume 17*, 1-11.

Lal, R. (2001). Soil degradation by erosion. Land degradation & development, 12(6), 519-539.

Lan, Y. Zhang, H. Lacey, R. Hoffmann, W. C. & Wu, W. (2009). Development of an integration sensor and instrumentation system for measuring crop conditions. *Agricultural Engineering International: CIGR Journal*, 11, pp.11-15.

Lemma, H., Admasu, T., Dessie, M., Fentie, D., Deckers, J., Frankl, A., ... & Nyssen, J. (2018). Revisiting lake sediment budgets: How the calculation of lake lifetime is strongly data and method dependent. *Earth Surface Processes and Landforms*, *43*(3), 593-607.

Li, Y., Ni, J., Yang, Q., & Li, R. (2006). Human impacts on soil erosion identified using land-use changes: a case study from the Loess Plateau, China. *Physical geography*, *27*(2), 109-126.

Liu, B. Y., Nearing, M. A., Shi, P. J., & Jia, Z. W. (2000). Slope length effects on soil loss for steep slopes. *Soil Science Society of America Journal*, *64*(5), 1759-1763.

Liu, K., Tang, G., Jiang, L., Zhu, A. X., Yang, J., & Song, X. (2015). Regional-scale calculation of the LS factor using parallel processing. *Computers & Geosciences*, *78*, 110-122.

Luvai, A., Obiero, J., & Omuto, C. (2022). Soil loss assessment using the revised universal soil loss equation (RUSLE) model. *Applied and Environmental Soil Science*, *2022*(1), 2122554.

Mahapatra, S. K., Reddy, G. O., Nagdev, R., Yadav, R. P., Singh, S. K., & Sharda, V. N. (2018). Assessment of soil erosion in the fragile Himalayan ecosystem of Uttarakhand, India using USLE and GIS for sustainable productivity. *Current Science*, *115*(1), 108-121. https://doi.org/10.18520/cs/v115/i1/108-121

Malleswara Rao, B. N., Umamahesh, N. V., & Reddy, G. T. (2005). GIS based soil erosion modelling for conservation planning of watersheds. *ISH Journal of Hydraulic Engineering*, *11*(3), 11-23. https://doi.org/10.1080/09715010.2005.10514

Masha, M., Yirgu, T., & Debele, M. (2021). Impacts of land cover and greenness change on soil loss and erosion risk in damota area districts, southern Ethiopia. *Applied and Environmental Soil Science*, *2021*, 1-14.

Maximus, J. K. (2025). Assessing watershed vulnerability to erosion and sedimentation: Integrating DEM and LULC data in Guyana's diverse landscapes. *HydroResearch*, *8*, 178-193.

McCool, D. K., Foster, G. R., & Weesies, G. A. (1997). Slope length and steepness factors (LS). In *Predicting soil erosion by water: A guide to conservation planning with the revised universal soil loss equation (RUSLE)* (Vol. 703). Washington, DC, USA: US Department of Agriculture.

Mekonnen, E., Kebede, A., Asfaw, S., & Feyissa, S. (2023). Optimizing soil erosion estimates of RUSLE model by analyzing land use/cover dynamics in upper Awash River Basin, Central Ethiopia. *Geomatics, Natural Hazards and Risk*, *14*(1), 2257363.

Melaku, B. S., Sefereh, E. Y., Emunu, M. H., & Wassie, D. Y. (2024). Application of communication strategies in the diffusion of agricultural innovations and technologies: the case of Amhara Regional Agricultural Research Institute, Ethiopia. *Cogent Social Sciences*, *10*(1), 2306704.

MoFED (Ministry of Finance and Economic Development) (2010). *Growth and transformation plan 2010/11-2014/15*. Volume I: Main text. Addis Ababa, Ethiopia: Ministry of Finance and Economic Development (MoFED), Federal Democratic Republic of Ethiopia.

Moges, D. M., & Bhat, H. G. (2018). An insight into land use and land cover changes and their impacts in Rib watershed, north-western highland Ethiopia. *Land degradation & development*, *29*(10), 3317-3330.

Molla, T., & Sisheber, B. (2017). Estimating soil erosion risk and evaluating erosion control measures for soil conservation planning at Koga watershed in the highlands of Ethiopia. *Solid Earth*, *8*(1), 13-25.

Morgan, R. P. C., Quinton, J. N., Smith, R. E., Govers, G., Poesen, J. W. A., Chisci, G., & Torri, D. (1998). The EUROSEM model. In *Modelling Soil Erosion by Water* (pp. 389-398). Springer Berlin Heidelberg.

Morgan, R. P. C. (2009). *Soil erosion and conservation*. John Wiley & Sons.

Musafiri, C. M., Kiboi, M., Macharia, J., Ng'etich, O. K., Kosgei, D. K., Mulianga, B., ... & Ngetich, F. K. (2022). Adoption of climate-smart agricultural practices among smallholder farmers in Western Kenya: do socioeconomic, institutional, and biophysical factors matter?. Heliyon, 8(1).

Mwanake, H., Mehdi-Schulz, B., Schulz, K., Kitaka, N., Olang, L. O., Lederer, J., & Herrnegger, M. (2023). Agricultural Practices and Soil and Water Conservation in the Transboundary Region of Kenya and Uganda: Farmers' Perspectives of Current Soil Erosion. *Agriculture*, *13*(7), 1434.

Mwanga, E. W., Shaibu, A. G., & Issaka, Z. (2024). Influence of long-term land use and land cover (LULC) changes on soil loss, sediment export, and deposition in the ungauged Bontanga watershed. *H2Open Journal*, *7*(1), 93-113.

Nachtergaele, F., van Velthuizen, H., Verelst, L., Wiberg, D., Henry, M., Chiozza, F., ... & Tramberend, S. (2023). *Harmonized World Soil Database version 2.0*. Food and Agriculture Organization of the United Nations.

Nigussie, A. B., Ayeled, G. T., Endalew, A., Miheretu, B. A., Amognehegn, A. E., Adamu, A. Y., & Karuppannan, S. (2025). Integrating Google Earth Engine and GIS for RUSLE-based soil erosion and sediment yield assessment in Borkena Watershed, Ethiopia. *J. Sediment. Environ.* (2025). https://doi.org/10.1007/s43217-025-00218-9

Nigussie, Z., Tsunekawa, A., Haregeweyn, N., Adgo, E., Nohmi, M., Tsubo, M., ... & Abele, S. (2017). Farmers' perception about soil erosion in Ethiopia. *Land degradation & development*, *28*(2), 401-411.

Nut, N., Mihara, M., Jeong, J., Ngo, B., Sigua, G., Prasad, P. V., & Reyes, M. R. (2021). Land use and land cover changes and its impact on soil erosion in Stung Sangkae catchment of Cambodia. *Sustainability*, *13*(16), 9276.

Nyesheja, E. M., Chen, X., El-Tantawi, A. M., Karamage, F., Mupenzi, C., & Nsengiyumva, J. B. (2019). Soil erosion assessment using RUSLE model in the Congo Nile Ridge region of Rwanda. *Physical Geography*, *40*(4), 339-360.

Panagos, P., Borrelli, P., Meusburger, K., Alewell, C., Lugato, E., & Montanarella, L. (2015a). Estimating the soil erosion cover-management factor at the European scale. *Land use policy*, *48*, 38-50.

Panagos, P., Borrelli, P., Meusburger, K., Yu, B., Klik, A., Jae Lim, K., ... & Ballabio, C. (2017). Global rainfall erosivity assessment based on high-temporal resolution rainfall records. *Scientific reports*, *7*(1), 1-12.

Patt, A., Suarez, P., & Gwata, C. (2005). Effects of seasonal climate forecasts and participatory workshops among subsistence farmers in Zimbabwe. *Proceedings of the National Academy of Sciences*, *102*(35), 12623-12628.

Pechanec, V., Mráz, A., Benc, A., & Cudlín, P. (2018). Analysis of spatiotemporal variability of C-factor derived from remote sensing data. *Journal of Applied Remote Sensing*, *12*(1), 016022-016022.

Pimentel, D., & Burgess, M. (2013). Soil erosion threatens food production. *Agriculture*, *3*(3), 443-463.

Regassa, A., Assen, M., Ali, A., & Gessesse, B. (2023). Major soil types. In The Soils of Ethiopia (pp. 77-110). Cham: Springer International Publishing.

Renard, K. G., & Freimund, J. R. (1994). Using monthly precipitation data to estimate the R-factor in the revised USLE. *Journal of hydrology*, *157*(1-4), 287-306.

Renard, K. G. (1997). Predicting soil erosion by water: a guide to conservation planning with the Revised Universal Soil Loss Equation (RUSLE). US Department of Agriculture, Agricultural Research Service.

Saravanan, S., Jegankumar, R., Selvaraj, A., Jennifer, J. J., & Parthasarathy, K. S. S. (2019). Utility of landsat data for assessing mangrove degradation in Muthupet Lagoon, South India. In *Coastal zone management* (pp. 471-484). Elsevier.

Sardari, M. R., Bazrafshan, O., Panagopoulos, T., & Sardooi, E. R. (2019). Modeling the impact of climate change and land use change scenarios on soil erosion at the Minab Dam Watershed. *Sustainability*, *11*(12), 3353.

Sartori, M., Philippidis, G., Ferrari, E., Borrelli, P., Lugato, E., Montanarella, L., & Panagos, P. (2019). A linkage between the biophysical and the economic: Assessing the global market impacts of soil erosion. *Land use policy*, *86*, 299-312.

Sartori, M., Ferrari, E., M'Barek, R., Philippidis, G., Boysen-Urban, K., Borrelli, P., ... & Panagos, P. (2024). Remaining Loyal to Our Soil: A Prospective Integrated Assessment of Soil Erosion on Global Food Security. *Ecological Economics*, 108103.

Schmidt, S., Alewell, C., & Meusburger, K. (2018). Mapping spatio-temporal dynamics of the cover and management factor (C-factor) for grasslands in Switzerland. *Remote Sensing of Environment*, *211*, 89-104.

Schmidt, S., Tresch, S., & Meusburger, K. (2019). Modification of the RUSLE slope length and steepness factor (LS-factor) based on rainfall experiments at steep alpine grasslands. *MethodsX*, *6*, 219-229.

Selassie, G. Y., Anemut, F., & Addisu, S. (2015). The effects of land use types, management practices and slope classes on selected soil physico-chemical properties in Zikre watershed, North Western Ethiopia. Environmental Systems Research, 4(1), 7. doi: 10.1186/s40068-015-0027-0

Sharpley, A. N., & Williams, J. R. (Eds.). (1990). EPIC-erosion/productivity impact calculator: 1. Model documentation.

Shi, Z. H., Cai, C. F., Ding, S. W., Wang, T. W., & Chow, T. L. (2004). Soil conservation planning at the small watershed level using RUSLE with GIS: a case study in the Three Gorge Area of China. *Catena*, *55*(1), 33-48.

Shiferaw, A. (2012). Estimating soil loss rates for soil conservation planning in the Borena Woreda of South Wollo Highlands, Ethiopia. *Journal of Sustainable Development in Africa*, *13*(3), 87-106.

Shulstad, R. N., & May, R. D. (1980). Conversion of noncropland to cropland: the prospects, alternatives, and implications. *American Journal of Agricultural Economics*, *62*(5), 1077-1083.

Sikka, A. K., & Sharda, V. N. (2002, May). Land and water care through participatory watershed management in India: An overview. In *Proceedings of 12th ISCO Conference, Beijing, China* (Vol. 26731).

Siraw, Z., Bewket, W., & Adnew, M. (2018). Effects of Community-Based Watershed Development on Soil Properties in the Northwestern Highlands of Ethiopia. *Malaysian Journal of Soil Science*, *22*.

Stone, R. P., & Hilborn, D. (2012). Universal soil loss equation (USLE) factsheet. *Ministry of Agriculture, Food and Rural Affairs order*, (12-051).

Taddese, G. (2001). Land degradation: a challenge to Ethiopia. *Environmental management*, *27*, 815-824.

Tamene, L., & Le, Q. B. (2015). Estimating soil erosion in sub-Saharan Africa based on landscape similarity mapping and using the revised universal soil loss equation (RUSLE). *Nutrient cycling in agroecosystems*, *102*, 17-31.

Tamene, L., Abera, W., Demissie, B., Desta, G., Woldearegay, K., & Mekonnen, K. (2022). Soil erosion assessment in Ethiopia: A review. Journal of Soil and Water Conservation, 77(2), 144-157.

Taye, G., Poesen, J., Wesemael, B. V., Vanmaercke, M., Teka, D., Deckers, J., ... & Haregeweyn, N. (2013). Effects of land use, slope gradient, and soil and water conservation structures on runoff and soil loss in semi-arid Northern Ethiopia. *Physical Geography*, *34*(3), 236-259.

Tesfaye, G., Assefa, A., & Kidane, D. (2017). Runoff, sediment load and land use/cover change relationship: the case of Maybar sub-watershed, South Wollo, Ethiopia. *International journal of river basin management*, *15*(1), 89-101.

Tesfaye, S., Taye, G., Birhane, E., & van der Zee, S. E. (2021). Spatiotemporal variability of ecosystem water use efficiency in northern Ethiopia during 1982–2014. *Journal of Hydrology*, *603*, 126863.

Tessema, Y. M., Jasińska, J., Yadeta, L. T., Świtoniak, M., Puchałka, R., & Gebregeorgis, E. G. (2020). Soil loss estimation for conservation planning in the welmel watershed of the Genale Dawa Basin, Ethiopia. *Agronomy*, *10*(6), 777.

Tian, P., Zhu, Z., Yue, Q., He, Y., Zhang, Z., Hao, F., ... & Liu, M. (2021). Soil erosion assessment by RUSLE with improved P factor and its validation: Case study on mountainous and hilly areas of Hubei Province, China. *International Soil and Water Conservation Research*, *9*(3), 433-444.

Tian, Y., Jiang, G., Wu, S., Zhou, D., Zhou, T., Tian, Y., & Chen, T. (2023). Cropland-grassland use conversions in the agro-pastoral areas of the Tibetan Plateau: Spatiotemporal pattern and driving mechanisms. *Ecological Indicators*, *146*, 109819.

Tiffen, M., & Mortimore, M. (1992). Environment, population growth and productivity in Kenya: a case study of Machakos District. *Development Policy Review*, *10*(4), 359-387.

Tittonell, P., Piñeiro, G., Garibaldi, L. A., Dogliotti, S., Olff, H., and Jobbagy, E. G. (2020). Agroecology in large scale farming—A research agenda. Front. Sustain. Food Syst. 214, 584605. doi:10.3389/fsufs.2020.584605

Tiwari, A. K., Risse, L. M., & Nearing, M. A. (2000). Evaluation of WEPP and its comparison with USLE and RUSLE. *Transactions of the ASAE*, *43*(5), 1129-1135.

Tsendbazar, N., Herold, M., Lesiv, M., & Fritz, S. (2018). Copernicus Global Lan d Operations: Validation Report of Moderate Dynamic Land Cover, Collection 100 M. *Version*, *1*, 68.

Tucker, C. J. (1979). Red and photographic infrared linear combinations for monitoring vegetation. *Remote sensing of Environment*, *8*(2), 127-150.

USGS. EarthExplorer. Available online: https://earthexplorer.usgs.gov/ (accessed on 20 June 2022).

Vanmaercke, M., Panagos, P., Vanwalleghem, T., Hayas, A., Foerster, S., Borrelli, P., ... & Poesen, J. (2021). Measuring, modelling and managing gully erosion at large scales: A state of the art. *Earth-Science Reviews*, *218*, 103637.

Wang, X., Song, K., Wang, Z., Li, S., Shang, Y., & Liu, G. (2024). Effects of land conversion to cropland on soil organic carbon in montane soils of Northeast China from 1985 to 2020. *Catena*, *235*, 107691.

Wang, Z., & Su, Y. (2020). Assessment of soil erosion in the Qinba Mountains of the southern Shaanxi Province in China using the RUSLE model. *Sustainability*, *12*(5), 1733.

Wani, S. P., Singh, H. P., Sreedevi, T. K., Pathak, P., Rego, T. J., Shiferaw, B., & Iyer, S. R. (2003). Farmer-participatory integrated watershed management: Adarsha watershed, Kothapally India. Case 7.

Wardlow, B. D., Egbert, S. L., & Kastens, J. H. (2007). Analysis of time-series MODIS 250 m vegetation index data for crop classification in the US Central Great Plains. Remote sensing of environment, 108(3), 290-310.

Wei J.B., Xiao D.N., Zeng H., Fu Y.K. (2008): Spatial variability of soil properties in relation to land use and topography in a typical small watershed of the black soil region, northeastern China. Environmental Geology, 53: 1663–1672.

Welde, K., & Gebremariam, B. (2017). Effect of land use land cover dynamics on hydrological response of watershed: Case study of Tekeze Dam watershed, northern Ethiopia. *International Soil and Water Conservation Research*, *5*(1), 1-16.

Mera, G. A. (2018). Drought and its impacts in Ethiopia. *Weather and climate extremes*, *22*, 24-35.

Wezel, A., Bellon, S., Doré, T., Francis, C., Vallod, D., & David, C. (2009). Agroecology as a science, a movement and a practice. A review. *Agronomy for sustainable development*, *29*, 503-515.

Wischmeier, W. H., & Smith, D. D. (1978). Predicting rainfall erosion losses: a guide to conservation planning (No. 537). Department of Agriculture, Science and Education Administration.

Woldemariam, A. D., Ddumba, S. D., & Addis, H. K. (2024). Modeling Sediment Yield with Current and Projected Climatic Scenarios in Andit Tid Watershed, Central Highland of Ethiopia. *Journal of Agriculture and Environment for International Development (JAEID)*, *118*(2), 83-118.

Yamaguchi, T., Kishida, K., Nunohiro, E., Park, J. G., Mackin, K. J., Hara, K., ... & Harada, I. (2010). Artificial neural networks paddy-field classifier using spatiotemporal remote sensing data. *Artificial life and robotics*, *15*, 221-224.

Yang, Y., Zhu, J., Zhao, C., Liu, S., & Tong, X. (2011). The spatial continuity study of NDVI based on Kriging and BPNN algorithm. *Mathematical and Computer Modelling*, *54*(3-4), 1138-1144.

Zanaga, D., Van De Kerchove, R., Daems, D., De Keersmaecker, W., Brockmann, C., Kirches, G., ... & Arino, O. (2022). ESA WorldCover 10 m 2021 v200. https://doi.org/10.5281/zenodo.7254221

Zhang, W., Hu, G., Dang, Y., Weindorf, D. C., & Sheng, J. (2016). Afforestation and the impacts on soil and water conservation at decadal and regional scales in Northwest China. Journal of Arid Environments, 130, 98-104.

Zhang, X., Lark, T. J., Clark, C. M., Yuan, Y., & LeDuc, S. D. (2021). Grassland-to-cropland conversion increased soil, nutrient, and carbon losses in the US Midwest between 2008 and 2016. *Environmental Research Letters*, *16*(5), 054018.

Zhao, G., Mu, X., Wen, Z., Wang, F., & Gao, P. (2013). Soil erosion, conservation, and eco-environment changes in the Loess Plateau of China. *Land Degradation & Development*, *24*(5), 499-510.

Zhao, J., Feng, X., Deng, L., Yang, Y., Zhao, Z., Zhao, P., ... & Fu, B. (2020). Quantifying the effects of vegetation restorations on the soil erosion export and nutrient loss on the Loess Plateau. *Frontiers in Plant Science*, *11*, 573126.